Aus der Klinik und Poliklinik für Dermatologie und Allergologie der

Ludwig-Maximilians-Universität München

Vorstand: Prof. Dr. med. Dr. h. c. G. Plewig

Human checkpoint proteins hRad9, hHus1, and hRad1 form a DNA damage-responsive complex

Dissertation

zum Erwerb des Doktorgrades der Medizin

an der Medizinischen Fakultät

der Ludwig-Maximilians-Universität zu München

vorgelegt von

Elias Volkmer

aus

München

2004

Mit Genehmigung der Medizinischen Fakultät

der Universität München

1. Berichterstatter:	Prof. Dr. med. Dr. h. c. G. Plewig
2. Berichterstatter:	Prof. Dr. med. P. Becker
1. Mitberichterstatter:	Priv. Doz. Dr. med. M. Kretzler
2. Mitberichterstatter:	Prof. Dr. med. D. J. Schendel
Mitbetreuung durch die promovierten Mitarbeiter:	Dr. med. E. Bornhövd
	Dr. med. T. Herzinger
Dekan:	Prof. Dr. med. Dr. h. c. K. Peter
Tag der mündlichen Prüfung:	04.11.2004

Für Martha Noemi

Content

1 Introduction

1.1 The genome is exposed to DNA-damaging agents

The genomes of all life forms are constantly exposed to DNA-damaging agents such as background ionizing radiation (IR), ultraviolet light (UV), and free oxygen radicals (Hoeijmakers, 2001). Medical diagnostic methods like radiographs or CT scans, and therapeutic strategies like chemotherapy and radiotherapy increase the exposure of humans to genotoxins. Exposure to genotoxins results in DNA damage. If not repaired, DNA lesions may be replicated during S phase or segregated into daughter cells during cell division, thus irreversibly establishing mutations in the individuals genome (Pages and Fuchs, 2002). Mutations may induce malignant transformation of single cell clones and cancer development (Bishop, 1991). Cells have therefore evolved mechanisms to accurately respond to DNA damage. When DNA is damaged, cells mount a well orchestrated response that includes cell cycle arrest and activation of DNA repair, thus promoting stability of the genome (Elledge, 1996; Weinert, 1998; Longhese, 1998). Genetic defects within these protection mechanisms may dramatically increase the rate of mutation, promoting genomic instability and the process of carcinogenesis (Hoeijmakers, 2001).

1.2 Genomic instability is an important factor in carcinogenesis

Genomic instability is now accepted as an important factor of carcinogenesis. It is defined as abnormal accumulation of mutations and cytogenetic alterations (Morgan et al., 1996; Hartwell, 1992). Nowell first suggested that genomic instability could initiate cancer development by promoting the evolution of increasingly abnormal tumor subpopulations (Nowell, 1976). The latter identification of oncogenes and tumor suppressor genes has demonstrated that single genetic defects may indeed trigger and even cause cancer (Hunter, 1991; Marshall, 1991). In support of Nowell's hypothesis, a sequential order of specific mutations has been described for several human tumors. Colorectal carcinomas, for example, typically exhibit inactivating mutations within the *APC* tumor suppressor gene followed by activating mutations of the *K-Ras* oncogene, loss of the active *DCC* tumor suppressor gene and finally the loss of functional *p53* (Fearon and Vogelstein, 1990). Because the inactivation of tumor suppressor genes (*APC*, *DCC*, *p53*) requires mutation of both alleles, at least seven mutations must take place for the colorectal cancer to develop. Similar sequential genetic

alterations were reported for lymphocytic cancers, malignant melanoma, and small cell lung cancer (Christians et al., 1995). Loeb validated Nowell's hypothesis showing that a normal cell endures no more than 2-3 mutations in an average life span, which can not account for the 6-7 mutations that are statistically required to set off malignant proliferation. He postulated that early in carcinogenesis mutations in key genes providing proper functions of DNA metabolism such as DNA repair, segregation, replication, and cell cycle control arise that increase the acquisition rate of spontaneous mutations, suggesting that cancer is a genetic multi-step disease (Loeb, 1991). Taken together, these studies suggest that defects in genes that ensure accurate DNA metabolism and provide genomic stability play a key role in cancer development.

Given that genomic instability is a central driving force behind malignant transformation, there has been significant interest in determining the molecular mechanisms that maintain genomic stability. Studies in yeast revealed different classes of genetic defects that lead to genomic instability. These include defects in DNA repair genes as well as in checkpoint control genes (Hartwell, 1992; Kaufmann et al., 1997), suggesting that these are the two key mechanisms in prevention of genomic instability and cancer.

1.3   Defects in DNA repair mechanisms cause genomic instability

The most evident class of DNA damage response mechanisms expected to influence genetic stability are DNA repair mechanisms. Different repair systems constantly scan the DNA to localize and repair specific types of DNA damage (Yu, 1999; Rosen, 1999; Lindahl and Wood, 1999). UV-induced thymidine-dimers, for example, are mainly repaired by excision repair (Sancar, 1994). Mismatches induced by polymerases can be readily repaired by DNA mismatch repair (Peltomaki, 2001; Hsieh, 2001). However, repair of DNA double strand breaks is less well understood. These breaks can be repaired with high fidelity by homologous recombination pathways and by error prone non-homologous end-joining pathways. Until recently, mammalian cells were thought to rely predominantly on non-homologous repair mechanisms; however, recent work has now shown that homologous repair also occurs (Jackson, 2002). It is evident that defects within these repair mechanisms influence genome stability. It has been postulated that defects in repair genes may generate an increased rate of

overall mutations and, as a result, an elevated probability of oncogenic mutations (Loeb, 1991; Hoeijmakers, 2001). This hypothesis has been repeatedly verified.

1.3.1　Xeroderma pigmentosum

The hereditary instability syndrome Xeroderma pigmentosum (XP) provides proof for repair genes being beneficial for maintenance of genomic stability. This autosomal-recessive disease is characterized by hypersensitivity to UV light and an early onset of cutaneous malignancies (malignant melanoma, basal cell and squamous cell carcinoma). Several genes identifying individual XP loci have been cloned. Defects within these genes generally impair the initial steps of nucleotide excision repair (de Boer and Hoeijmakers, 2000; Wood, 1995). Hence, a gene defect and subsequent dysfunction of a specific DNA repair mechanism trigger the accumulation of mutations and ultimately the development of cancer.

1.3.2　Nijmegen breakage syndrome

Studies on the inherited disorder Nijmegen breakage syndrome (NBS) validated the findings gained from XP. NBS patients exhibit microcephaly, immunodeficiency, and a higher incidence of hematopoietic malignancy. Cells derived from NBS patients are more sensitive to IR and display higher levels of spontaneous and induced chromosomal instability (Weemaes et al., 1981; van der Burgt et al., 1996). NBS cells also fail to induce G1-S and S phase cell cycle arrest that usually follows DNA damage (Tauchi et al., 2002). The disease NBS is caused by genetic defects in the *NBS1* gene, which was mapped to the gene locus encoding the protein p95 (Varon et al., 1998). p95 was shown to be one of five molecules of a DNA double-strand break repair complex. The function of the repair complex is impaired in cells from NBS patients, which strongly suggests that dysfunction of a DNA repair mechanism causes genomic instability and cancer predisposition (Petrini et al., 1997). The fact that defects in a gene required for DNA repair also lead to defects in DNA damage-induced cell cycle arrest, suggests that these two mechanisms functionally overlap or operate in close functional proximity.

1.3.3 BRCA1

Women with germ-line mutations of the *BRCA1* gene exhibit predisposition to breast and ovarian cancers (Feunteun and Lenoir, 1996). This suggests an impact of the BRCA1 gene product in maintenance of genomic integrity. However, it was not clear what role BRCA1 played in this process. A role in DNA repair has been proposed, but BRCA1 has also been involved in cell cycle control (Paterson, 1998; Xu et al., 1999). Both functions would suffice individually to explain the carcinogenic effect of BRCA1 mutations. Although it remains unclear whether BRCA1's role in DNA repair or its role in cell cycle control or a combination of the two is responsible for the elevated risk of cancer, these studies suggest that disruption of DNA damage-activated cell cycle arrest and/or DNA repair leads to increased cancer susceptibility.

1.4 Cell cycle checkpoints also have an impact on genomic stability

In view of their apparent participation in DNA damage responses, DNA damage-induced cell cycle arrest pathways gained importance in cancer research (Hartwell and Kastan, 1994). During proliferation, every eucaryotic cell replicates DNA and divides in a series of coordinated events that constitute the cell cycle (G1 to S to G2 to M). Cell cycle progression is carried out by a cascade of protein phosphorylations mediated by cyclin-dependent kinases (CDKs). At each cell cycle boundary, e.g., G1-S or G2-M, CDKs associate with their corresponding, transiently expressed cyclins. The active cyclin-CDK complex then relays the cell to the next stage of the cell cycle (Collins et al., 1997). If the conditions for transition are not appropriate, signaling cascades are activated that inhibit CDK function. This delays progression through the cell cycle until the disturbance has been cleared, ensuring fidelity of previous cell cycle events. Referring to their supervisory function, these signaling cascades were termed cell cycle checkpoints (Hartwell and Weinert, 1989). In a model, checkpoints consist of a sensor that detects irregularities and a signaling cascade that enhances and transmits the signal to an effector. The effector then relays the signal to the cell cycle machinery to delay cell cycle progression (Carr, 1996; Weinert, 1997; Fig. A).
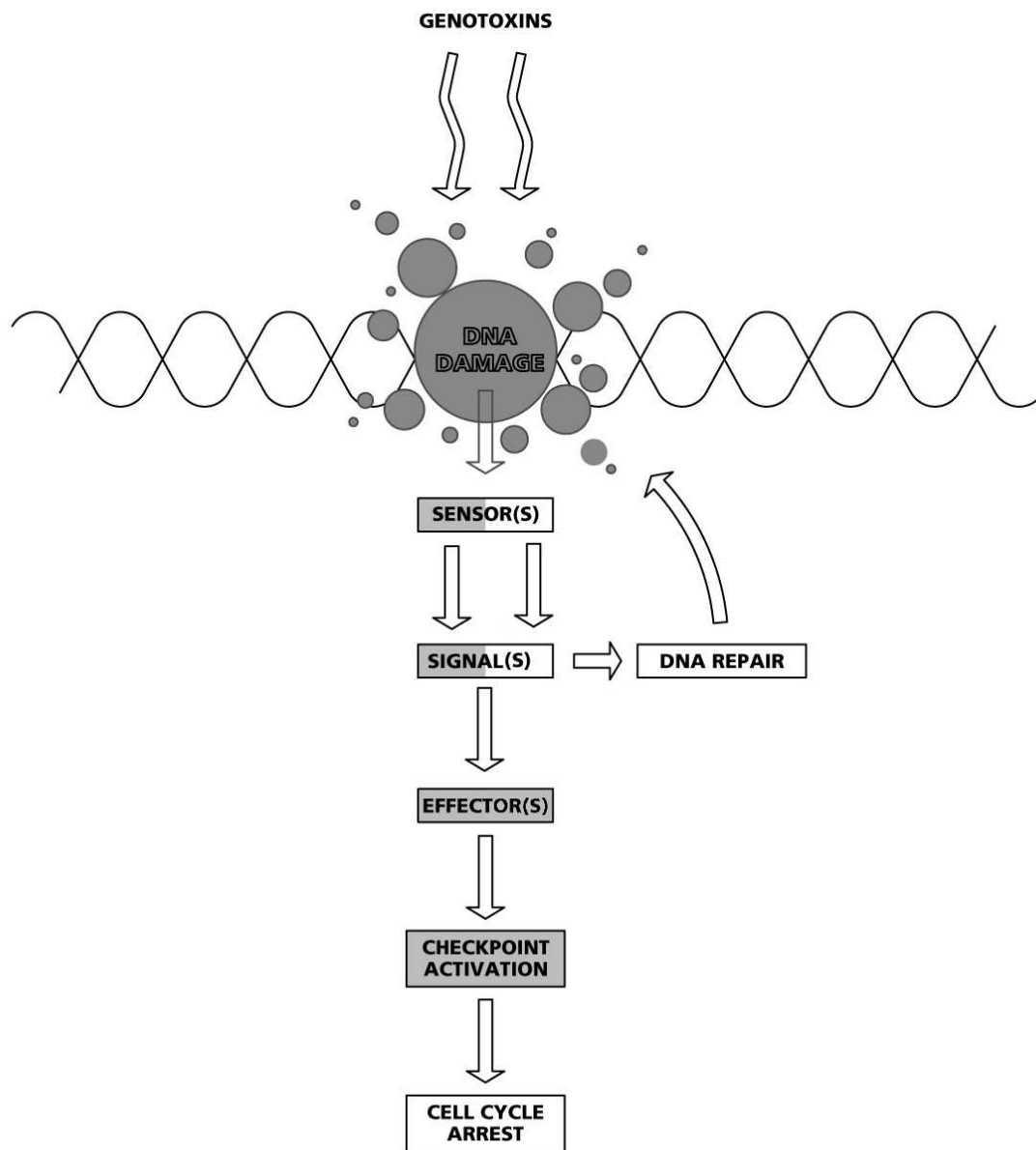
Figure A. Genotoxins induce DNA damage, which activates cellular signaling cascades consisting of sensor(s), signal(s), and effector(s). These signaling pathways mediate the cellular DNA damage response. While checkpoint activation leads to cell cycle arrest, parallel pathways initiate DNA repair.

Today, at least four different checkpoints are known that monitor DNA metabolism in eucaryotes: The G1-S checkpoint halts the cell at the G1-S transition. The S-phase progression checkpoint slows down progression through S-phase. The G2-M checkpoint and the S/M checkpoint prevent segregation of damaged or incompletely replicated DNA (Weinert, 1998; Elledge, 1996). DNA damage checkpoints thus form part of the cellular DNA damage

response helping to preserve the integrity of the genome and promote genomic stability (Fig. B).
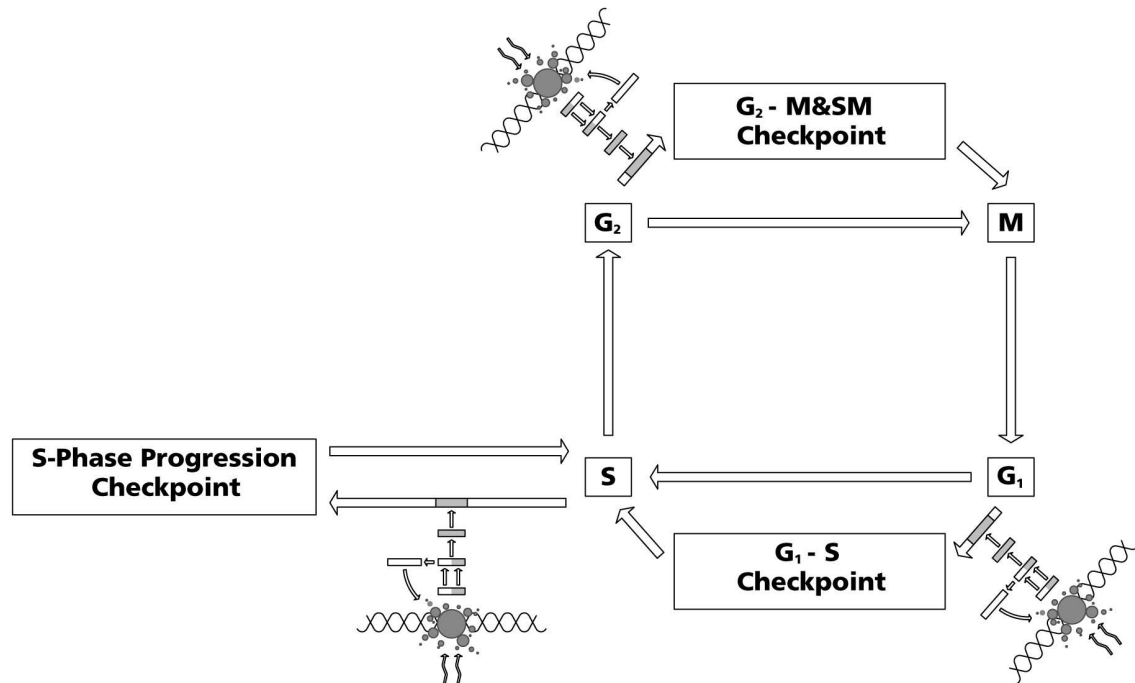
Figure B. The somatic cell cycle is defined by the period between two mitotic events. It is divided into M-phase, G1-phase, S-phase, and G2-phase. If DNA damage is detected, signal-transduction pathways lead to checkpoint activation. At least four different checkpoints monitor DNA metabolism in eucaryotes: The G1-S checkpoint, the S-phase progression checkpoint, the G2-M checkpoint, and the S/M checkpoint.

As cell cycle checkpoints are not essential for cell survival their significance for genomic stability has been less apparent. The impact of checkpoint defects, however, may be all the more: genetic defects in checkpoint-regulating genes may disrupt checkpoint activation in response to altered DNA metabolism. Depending upon the localization of the defect, various types of damage are to be expected: override of the G1-S checkpoint, for example, would generate mutations as a consequence of premature DNA replication. Loss of the G2-M checkpoint would result in gross chromosomal aberrations and loss of genetic material. Any DNA damage responsive checkpoint gene deficiency in combination with induced DNA damage, e.g., by IR would result in an elevation of mutagenic events in a cell. These notions support an implication of genetic checkpoint defects in genomic instability and cancer development. Interestingly, unlike normal cells, tumor cells often exhibit checkpoint defects when exposed to DNA damage (Hartwell et al., 1994). Although we know little about how

these checkpoints function in humans, their impact on genomic stability and their association with cancer underscore the importance of studying these mechanisms intensively.

1.4.1   p53

There is increasing evidence that tumor suppressor genes encode proteins that regulate cell cycle control mechanisms (Collins et al., 1997). As a result, the first breakthroughs in the search for checkpoint genes causing genomic instability were achieved by the analysis of known tumor suppressor genes. The most prominent discovery was the tumor suppressor gene *p53*. p53 is a sequence specific DNA-binding transcriptional activator (Levine, 1997). It up-regulates expression of several genes involved in either G1 arrest or apoptosis. DNA damage or inappropriate growth stabilize p53 metabolically and consequently increase cellular p53 levels (Donehower, 1997). p53-dependent genes then mediate cell cycle delay at the G1-S transition or, alternatively, induce apoptosis (Kastan et al., 1995).

Effects of defective p53 have been studied in the familial cancer syndrome Li-Fraumeni (LF). This autosomal-recessive disease is caused by homozygous *p53* mutations. LF patients exhibit an early onset of multiple primary tumors, indicating that functional inactivation of p53 plays a significant role in tumorigenesis (Tainsky et al., 1995). Knock out mice with a homozygous *p53*-null mutation are viable, and like LF patients exhibit cancer development very early in life (Donehower et al., 1997). On a cellular level, p53-deficiency (p53$^-$) inhibits initiation of the G1 checkpoint following DNA damage, and p53-deficient cells are unable to undergo apoptosis in response to irreparable DNA damage. Lack of the p53 gene allows a high intrinsic rate of genomic alterations such as translocations, chromosomal aberrations, aneuploidy, gene amplification, and mutations (Tainsky et al., 1995). This clearly demonstrates the importance of unaltered p53 function in regard to genomic stability and suggests that unaltered checkpoint function and induction of apoptosis are crucial in prevention of carcinogenesis.

However, the mutation of p53 often occurs very late in the stepwise process of tumorigenesis, e.g., colorectal cancer, and G2-M and S-phase checkpoints are only partially

affected in p53-deficient cells. It is therefore reasonable to expect other, p53-independent checkpoint controls to play a role in carcinogenesis.

1.4.2   Ataxia telangiectasia

The study of a different human instability syndrome termed ataxia telangiectasia (AT) reinforced the role of checkpoints in genome maintenance and their impact on cancer, and it further pointed toward p53-independent checkpoints as important factors in DNA damage response. Homozygote patients with this rare, autosomal recessive genetic disorder suffer from cerebellar ataxia, oculocutaneous telangiectasia, immunodeficiency, premature aging, and an approximately 100-fold increased risk of cancer, particularly leukemias and lymphomas. Heterozygous carriers (approximately 1.4% of the caucasian US population) have a relative risk of cancer of 2.3 (men) to 3.1 (women), with an exceptionally high relative risk of breast cancer of 6.8 (Swift et al., 1987, 1994, 1997). It has been calculated that as many as 6.6% of all breast cancers in the US may occur in women heterozygous for AT (Athma et al., 1996). The defective gene in AT has recently been identified, and designated *AT-M*utated or *ATM* (Savitsky et al., 1995). The ATM phenotype corresponds to some extent to the phenotype of NBS. Cells deriving from AT patients exhibit elevated sensitivity to IR and radiomimetic drugs and display chromosomal instability and abnormal genetic recombination (Gatti, 1991). Additionally, AT cells are defective in the induction of G1-S, S-phase, and G2 checkpoints in response to IR. The G1-S checkpoint deficiency is due, at least in part, to suboptimal induction of p53. In a signaling cascade activated by DNA damage, ATM acts upstream of p53 and there is compelling evidence that the ATM kinase directly phosphorylates p53 *in vivo* in response to DNA damage induced by IR (Canman et al., 1998). AT cells also fail to induce p53-independent checkpoints indicating that the ATM lies far upstream in the cascade of detection and/or mediation of DNA damage signals. The above suggests that checkpoint defects are responsible for the AT related symptoms. Lately, ATM dysfunction has been associated with decreased DNA double strand break repair (Maser et al., 1997; Petrini et al., 1997) suggesting a role for ATM in induction of DNA repair. These studies suggest an integral role for ATM in cellular DNA damage responses.

The cloning of the *ATM* gene unveiled an additional striking feature of checkpoint genes: *ATM* has significant sequence homology to genes in the yeast *Schizosaccharomyces pombe* (*sprad3*), *Saccharomyces cerevisiae* (*scmec1* and *sctel1*) and *Drosophila melanogaster* (*MEI-41*), suggesting evolutionary conservation of checkpoint genes from yeast to humans (Savitsky, 1995; Zakian, 1995; Hoekstra, 1997). Because the homology extends to the PI-3 kinase related region, they were all termed PI-3 kinase related kinases or PIKKs. So far all PIKKs are associated with functions in DNA damage response. For example, scMec1 and spRad3 both regulate checkpoint activation in response to DNA damage. Defects in the *sprad3* and *scmec1* genes, like defects in *ATM*, also sensitize the organisms to radiation and radiomimetic drugs, additionally suggesting conservation of functional aspects of checkpoint pathways (Carr, 1997).

1.5 *Schizosaccharomyces pombe* serves as a model system to study cell cycle control mechanisms

The similarities of genetic components in yeast and humans extend beyond these kinases. The fission yeast *S. pombe* has served for many years as a model system to study cell cycle control mechanisms and DNA damage-activated checkpoint responses. Large collections of yeast mutants that are sensitive to IR, UV light, and radiomimetic drugs have been identified in the last two decades (Elledge, 1996; Paulovich et al., 1997). With the advent of molecular biology and the genome sequencing projects, the genes responsible for the radiation sensitive phenotypes have been cloned. Many of the genes causing increased sensitivity are known as rad genes, for "radiosensitive" genes. Some of them are clearly involved in DNA repair mechanisms. Some gene products, however, regulate G2 and S-phase checkpoint delays along with G1 arrest, suggesting a critical role for checkpoint genes in cellular DNA damage responses (Kostrub et al., 1998; Longhese et al., 1998; Volkmer and Karnitz, 1999).

In *S. pombe* there are at least six genes (*sprad1*, *sprad3*, *sprad9*, *sprad17*, *sprad26*, and *sphus1*) that are crucial for induction of the G2 delays in response to DNA damage and replication blocking agents (al-Khodairy et al., 1994). Defects in one or more of these genes render the yeast more sensitive to genotoxic agents (Rowley et al., 1992; al-Khodairy and
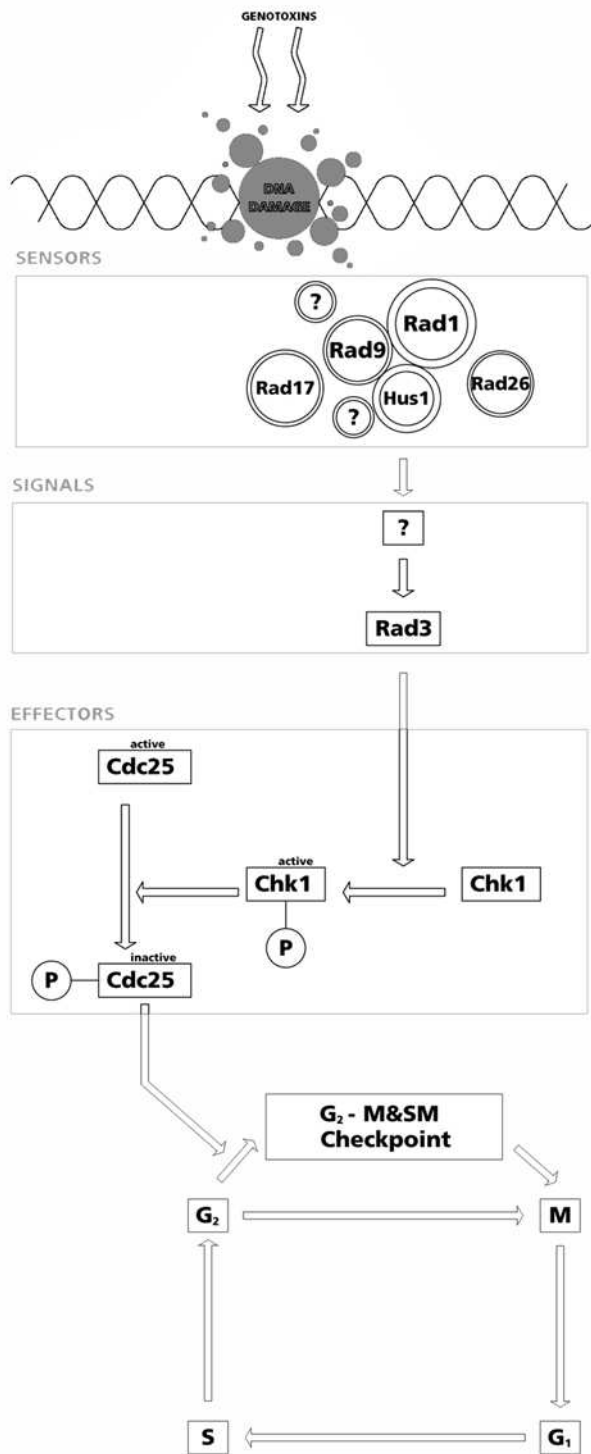
Figure C. In a tentative model of G2 checkpoint activation an uncharacterized sensor recognizes DNA damage. The sensor(s) then interface with at least two kinases: the Rad3 kinase and the Chk1 kinase. The Rad3 kinase activates Chk1 by phosphorylation. This phosphorylation requires the five other checkpoint genes (*rad1*, *rad9*, *rad17*, *rad26*, and *hus1*), suggesting that their gene products operate upstream of Rad3. Chk1 then inactivates Cdc25, a cell cycle phosphatase in *S. pombe*, which prevents cell cycle transition through the G2-M boundary.

Carr, 1992; Enoch et al., 1992). Mutations in these genes do not affect cell cycle progression, suggesting that they regulate a common pathway of DNA damage response but are not essential under normal growth conditions (Collins et al., 1997). Based on genetic and biochemical evidence, a tentative pathway has been proposed for how fission yeast respond to DNA damage (Fig. C). Although still in their infancy, these studies suggest that an uncharacterized sensor recognizes DNA damage. Once activated, the sensor(s) then interfaces with a signaling pathway that is composed of at least two kinases: the Rad3 kinase and the Chk1 kinase. The Rad3 kinase lies upstream of and is required for Chk1 phosphorylation. This phosphorylation, in turn, activates Chk1 and requires the five other checkpoint genes (*rad1*, *rad9*, *rad17*, *rad26*, and *hus1*), suggesting that their gene products operate upstream of Rad3 (Carr, 1996; Weinert, 1997). Once activated, Chk1 phosphorylates Cdc25, a cell cycle phosphatase required for the activation of the cyclin-dependent kinase Cdc2 in *S. pombe*. This finally prevents cell cycle transition through the G2-M boundary, thus linking DNA damage recognition to the cell cycle progression machinery (Furnari et al., 1997). Although genetic evidence in yeast and humans demonstrates the importance of the Rad3 and the ATM kinase, we have little understanding of how these kinases are activated by DNA damage or what regulates their activities. The other rad gene products, which are genetically required for Rad3 function, may be key components that link the kinases Rad3 and Chk1 to DNA damage.

1.5.1 Human homologs of the S. pombe checkpoint genes have been identified

Within the last five years, a panel of potential human homologs of the *S. pombe* checkpoint genes has been identified and molecularly cloned, further underscoring the similarities between yeast and humans (Table 1). This group of novel human genes includes homologs of *sprad1* (*hRAD1*), *sprad3* (*ATM*), *sprad9* (*hRAD9*), *sprad17* (*hRAD17*), *sphus1* (*hHUS1*), and *spchk1* (*hCHK1*), all of which display a high degree of evolutionary conservation (Udell et al., 1998; Savitsky et al., 1995; Lieberman et al., 1996; Parker et al., 1998; Kostrub et al., 1998; Sanchez et al., 1997). Some of these human homologs partially restore checkpoint function if expressed in the corresponding checkpoint mutant yeast cells, suggesting that the genes are functionally conserved (O'Connell et al., 2000). The similarity of

gene sequence and the partial conservation of function raises speculations about the function of human rad genes and their possible impact on the process of carcinogenesis.

Table 1. Yeast homologs of human checkpoint genes

Human	*S. pombe*	*S. cerevisiae*	**Activity**
hRAD1	*sprad1*	*scrad17*	Exonuclease*
ATM/ATR	*sprad3*	*scmec1/sctel1*	PIKK*
hRAD9	*sprad9*	*scddc1*	*
hRAD17	*sprad17*	*scrad24*	RFC-related*
hRAD26	*sprad26*	-	*
hHUS1	*sphus1*	-	*
hCHK1	*spchk1*	-	PK
hCDC25	*spcdc25*	-	Phosphatase
hCDC2	*spcdc2*	-	CDK

* known to be crucial for the DNA damage checkpoint in yeast

Assuming that, like in yeast, defects in a single checkpoint gene lead to abrogation of the G2 checkpoints, the effect in humans may be dramatic. DNA damage would no longer hinder the cells from progressing into mitosis creating a huge potential for development of mutated cells (Kaufmann et al., 1997). Inactivating mutations of rad genes may lead to increased rates of mutations and genomic instability as known for p53. Human checkpoint genes therefore have the potential to be tumor suppressors. Mapping of the human *RAD9* gene (*hRAD9*) located it to a region for loss of heterozygosity in cervical cancer cell lines, suggesting that *hRAD9* may be the causative tumor suppressor gene in this region (Lieberman et al., 1996). Likewise, the *hRAD1* gene is located in a region that is subject to loss of heterozygosity in several human malignancies including lung cancer (Parker et al., 1998). Even if rad genes were not tumor suppressors, they may still cause an increased rate of mutation

required for initiation of tumor development. Because they have a crucial impact on maintenance of genomic stability, heterozygous defects within rad genes may be responsible for inherited predisposition to cancer, as are some of the known tumor suppressors.

1.6   Clinical impact of checkpoint research

The aspect that renders investigation of alternative checkpoints clinically attractive is the potential of therapeutic exploitation of checkpoint research, for example for checkpoint-based chemotherapy. More than 50% of all human malignant tumors contain defective p53. Loss of p53 function disrupts the G1-S checkpoint, which generally increases radiosensitivity of cells. However, p53-dependent pathways also lead to apoptosis, and lack of p53 reduces the ability to induce apoptosis in response DNA damage, which renders the cells less sensitive to genotoxic agents, e.g., chemotherapeutic drugs. In some tumor cell lines, this effect dominates the phenotype and, as a consequence, these tumor cell lines have reduced chemosensitivity and radiosensitivity (Lutzker and Levine, 1996). In order to increase therapeutic tumor-cell killing, it has been tested whether substances that abrogate the G2 checkpoints preferentially radiosensitize p53$^-$ tumor cells by disrupting G2 checkpoints, which potentially compensate for the absence of the genoprotective G1-S checkpoint (Powell et al., 1995). Selective G2-checkpoint abrogators like UCN-01 (7-hydroxystaurosporine) increased killing of p53-deficient tumor cells by γ-irradiation (Wang et al., 1996). UCN-01 is currently undergoing clinical trials for cancer treatment (Sausville et al., 2001). Interestingly, the G2-checkpoint abrogation is mediated by inhibition of Chk1, suggesting that other checkpoint proteins may be potential targets for cancer therapy as well (Busby et al., 2000; Graves et al., 2000). To devise a rational search for additional substances of use in checkpoint-based chemotherapy, investigation of the molecular mechanisms underlying checkpoint function is necessary.

1.7   Aim of this study

In view of this potential importance of human rad genes in checkpoint control and possibly carcinogenesis, we have undertaken a cellular and molecular analysis of the novel human checkpoint proteins hRad9, hHus1, and hRad1 in K562 cells. Although these proteins have been identified, it is not yet clear how they regulate the responses of mammalian cells to DNA damage. Our aim was to determine whether and how hRad9, hHus1, and hRad1 are

involved in the basic molecular mechanisms of DNA damage response. Do they imitate molecular processes of yeast cells, suggesting conservation of checkpoint response from yeast to humans? To see whether the studies performed with human chronic myelogenous leukemia cells (K562) are representative for human skin cells, we performed identical experiments with human keratinocytes. As the skin is specifically exposed to UV irradiation, we analyzed, whether UV-induced DNA damage may differently affect hRad9-, hHus1-, and hRad1-dependent molecular responses. We thus elucidated molecular mechanisms underlying the function of human checkpoint proteins hRad9, hHus1, and hRad1 in K562 cells and in human keratinocytes. This study facilitates future progress in our understanding of human checkpoint function and may permit advances in the development of new strategies in cancer therapy.

2 Materials and methods

2.1 Chemicals and reagents

2.1.1   List of chemicals

α-HA monoclonal mAB	Babco, Berkeley, CA
α-AU1 monoclonal mAB	Babco, Berkeley, CA
α-FLAG monoclonal mAB	Kodak, New Haven, CT
α-GFP rabbit antiserum	Molecular Probes, Eugene, OR
Acrylamide	National Diagnostic, Atlanta, GA
Acrylamide/bis	Sigma, St. Louis, MO
Ammonium persulfate	Sigma, St. Louis, MO
Ampicillin	Sigma, St. Louis, MO
Aprotinin	Sigma, St. Louis, MO
Bacto yeast extract	Difco, Detroit, MI
Bacto tryptone	Difco, Detroit, MI
Bacto agar	Difco, Detroit, MI
β-Glycerophospate	Sigma, St. Louis, MO
Bovine serum albumin (BSA)	Sigma, St. Louis, MO
Bromophenol blue	IBI, New Haven, CT
Calcium chloride (CaCl)	Aldrich, Milwaukee, WI
Calf intestinal phosphatase (CIP)	Gibco BRL, Gaithersburg, MD
Cesium chloride (CsCl)	Boehringer Mannheim, Indianapolis, IN
EDTA	Sigma, St. Louis, MO
Ethanol (100%)	Sigma, St. Louis, MO
Ethidium bromide	Sigma, St. Louis, MO
Expand high fidelity PCR system	Boehringer Mannheim, Indianapolis, IN
Fetal calf serum (FCS)	Biofluids, Rockville, MD
Glacial acetic acid (GAA)	EM Science, Gibbstown, NJ
Glucose	Sigma, St. Louis, MO
Glycerol	Sigma, St. Louis, MO
Glycine	Sigma, St. Louis, MO
Guanidine HCl	BRL Life Technologies, Gaithersburg, MD
Hepes	Boehringer Mannheim, Indianapolis, IN
Horseradish peroxidase (HRP)	Amersham, Arlington Heights, IL
HRP-conjugated protein A	Amersham, Arlington Heights, IL
Hydrochloric acid (HCl)	J.T. Baker, Phillipsburg, NJ
Immobilon P membrane	Millipore, Bedford, MA
Kanamycin	Sigma, St. Louis, MO
KH_2PO_4	Sigma, St. Louis, MO
K_2HPO_4	Sigma, St. Louis, MO
LE agarose	FMC Bio Products, Rockland, MA
L-glutamine	Sigma, St. Louis, MO
Leupeptin	Sigma, St. Louis, MO
Lysozyme	Boehringer Mannheim, Indianapolis, IN
Magnesium chloride ($MgCl_2$)	Sigma, St. Louis, MO
2-β-Mercaptoethanol (2-ME)	Sigma, St. Louis, MO

Methanol (100%)	Sigma, St. Louis, MO
Microcystin-LR	Sigma, St. Louis, MO
Paraformaldehyde	Sigma, St. Louis, MO
PCR-ready human testes cDNA library	Clontech, San Diego, CA
Pepstatin	Sigma, St. Louis, MO
Potassium acetate (KAc)	Sigma, St. Louis, MO
Potassium chloride (KCl)	Sigma, St. Louis, MO
Propidium iodide (PI)	Sigma, St. Louis, MO
Protein A sepharose beads	Sigma, St. Louis, MO
Protein G sepharose beads	Sigma, St. Louis, MO
Polaroid film type 53 (4 x 5", b/w)	Polaroid Corporation, Cambridge, MA
Polyoxyethylene sorbitan monolaureate (TWEEN 20)	Sigma, St. Louis, MO
Qiagen QIAquick gel extraction kit	Qiagen, Santa Clarita, CA
Qiagen plasmid extraction kit	Qiagen, Santa Clarita, CA
Rabbit-anti-mouse IgG	Pierce, Rockford, IL
Rabbit-anti-mouse IgG, HRP-conjugated	Pierce, Rockford, IL
RPMI-1640 medium	Bio Whittaker, Walkersville, ML
Sodium acetate (NaAc)	Sigma, St. Louis, MO
Sodium azide (NaN$_3$)	Sigma, St. Louis, MO
Sodium chloride (NaCl)	Sigma, St. Louis, MO
Sodium dodecyl Sulfate (SDS)	Sigma, St. Louis, MO
Sodium fluoride (NaF)	Sigma, St. Louis, MO
Sodium hydroxide (NaOH)	Sigma, St. Louis, MO
Sodium orthovanadate (Na$_3$VO$_4$)	Fisher Scientific, Pittsburgh, PA
Sodium phosphate (Na$_2$HPO$_4$) anhydrous	Sigma, St. Louis, MO
Sodium phosphate (7H$_2$O)	Sigma, St. Louis, MO
Super signal chemilumenescent substrate	Pierce, Rockford, IL
Tetramethyl-1,2-diaminoethane (TEMED)	Sigma, St. Louis, MO
TnT quick coupled transcription/ translation system	Promega, Madison, WI
Trichloroacetic acid	EM Science, Gibbstown, NJ
Tris hydroxymethylaminoethane (TRIS)	Sigma, St. Louis, MO
TRIS HCl	Sigma, St. Louis, MO
Triton-X 100	Sigma, St. Louis, MO
Vectashield antifade mounting medium	Vector Laboratories, Burlingame, CA

2.1.2   Enzymes

2.1.2.1 Polymerase

Expand high fidelity polymerase	Boehringer Mannheim, Indianapolis, IN

2.1.2.2 Ligase

T4 DNA ligase   New England Biolabs, Beverly, MA

2.1.2.3 Restriction enzymes

Asc I   New England Biolabs, Beverly, MA
*Eco*R I   New England Biolabs, Beverly, MA
Xba I   New England Biolabs, Beverly, MA
Xho I   New England Biolabs, Beverly, MA

2.1.3   Epitope tags

AU-1   Amino Acid Sequence: DTYRYI
HA   Amino Acid Sequence: YPYDVPDYA
FLAG   Amino Acid Sequence: DYKDDDDK
GFP   Prasher et al., 1992

2.1.4   Plasmids

pcDNA3   Invitrogen, Carlsbad, CA
pEF-BOS-ΔRI   Mizushima et al., 1990
pET24a+   Novagen, Madison, WI
pGEX-KG   Guan and Dixon, 1991
pGFP-N1   Clontech, San Diego, CA

2.1.5   Genes

hRAD1   Udell et al., 1998
hRAD9   Lieberman et al., 1996
hHUS1   Kostrub et al., 1998

2.2   Instruments

2.2.1   Centrifuges and rotors

Ultracentrifuge L8-70 with
        NVT 65 rotor (r_{av}=72.2 mm)   Beckman, Palo Alto, CA
Microfuge R table top centrifuge with
        F 241.5 rotor (r_{av}=80 mm)   Beckman, Palo Alto, CA
J2-21 centrifuge with
        JA-17 rotor (r_{av}=123 mm)   Beckman, Palo Alto, CA

2.2.2   Other instruments

Bacteria cell incubator   Thelco, Pittsburgh, PA
Cell counter coulter counter ZM   Coulter Pharmaceutical, Inc., Palo Alto, CA
Confocal laser scanning
        microscope LSM510   Carl Zeiss Inc., Jena, Germany

^{137}Cs γ-irradiator	J.L. Shepard, San Fernando, CA
FS20 UVB lamp	Westinghouse, Pittsburgh, PA
WG-295 long pass UVC filter	Schott Glass Technologies, Duryea, PA
IL 443 UVB radiometer	International Light, Newburyport, MA
SEE 240 photodetector	International Light, Newburyport, MA
Electrophoresis unit Hoefer SE 600 series	Hoefer Scientific Instruments, San Francisco, CA
Electrophoresis unit Hoefer TE series transphor	Hoefer Scientific Instruments, San Francisco, CA
4 mm-electroporation cuvettes	BTX, San Diego, CA
Electroporator BTX T 820	BTX, San Diego, CA
Orbital shaker gene mate OS 350	Intermountain Scientific Corporation, Kaysville, UT
PCR thermocycler gene amp PCR system 9600	Perkin Elmer, Norwalk, CT
Power supply power pac 1000	Bio-Rad Laboratories, Hercules, CA
Polaroid MP 4+ gel camera	Polaroid Corporation, Cambridge, MA
Power supply power pac 200	Bio-Rad Laboratories, Hercules, CA
Safety stand BTX 630A	BTX, San Diego, CA
Tissue culture incubator 4535	Forma Scientific, Marietta, OH

2.3   Recipes

2.3.1   Buffers and solutions

30% Acrylamide stock for SDS-PAGE

300.0 g Acrylamide	(29.2%)
8.2 g Acrylamide/bis	(0.4%)

adjust the volume to 1027 ml with deionized water
- filter solution through a 0.45 μm filter to remove particles

Agarose gel loading buffer (100 ml of 5X stock)

- to 30 ml of deionized water, add:

50 ml glycerol	(50%)
10 ml of 50X TAE	(5X)
- add 500 μg SDS	(0.5%)
- add 250 μg bromophenol blue	(0.25%)

- adjust the volume to 100 ml with deionized water

GTE buffer (20 ml)

- to 10 ml of deionized water, add:

180 mg glucose	(50 mM)
0.4 ml of 2 M TRIS HCL, pH=8.0	(25 mM)
0.4 ml EDTA	(10 mM)

- adjust the volume to 20 ml with deionized water

EDTA (100 ml of 500 mM stock)

- to 50 ml deionized water, add:

18.6 g EDTA	(500 mM)

- adjust to pH 8.0 with concentrated HCl
- adjust the volume to 100 ml with deionized water

KAc solution (30 ml)
- to 18 ml of 5 M KAc, add: (3 M)
3.5 ml glacial acetic acid   (11.7%)
- adjust the volume to 30 ml with deionized water

Resolving gel buffer (1000 ml)
- to 750 ml of deionized water, add:
181.7 g TRIS   (1.5 M)
4 g SDS   (0.4%)
- adjust to pH 8.8 with concentrated HCl
- adjust the volume to 1000 ml with deionized water

Lysis buffer (500 ml)
- to 250 ml of deionized water, add:
25 ml HEPES   (50 mM)
5 g Triton X 100   (1%)
0.21 g NaF   (10 mM)
6.7 g $Na_4P_2O_7$ (30 mM)
15 ml of 5 M NaCl   (150 mM)
1 ml of 500 mM EDTA stock   (1 mM)
- adjust the volume to 500 ml with deionized water
- prior to use add freshly:
β-glycerophosphate to 10 mM   (10 mM)
Na_3VO_4 to 1 mM   (1 mM)
pepstatin A to 20 μg/ml   (20 μg/ml)
aprotinin to 10 μg/ml   (10 μg/ml)
leupeptin to 20 μg/ml   (20 μg/ml)
microcystin-LR to 40 μM   (40 μM)

Lysozyme solution
- to 2 ml of GTE buffer, add:
100 mg lysozyme   (5%)

NaOH/SDS buffer (34 ml)
- to 20 ml of deionized water, add:
680 μl of 10 N NaOH   (0.2 M)
3.4 ml of 10% SDS   (1%)
- adjust the volume to 34 ml with deionized water

PBS washing buffer (1000 ml of 10X stock)
- to 750 ml of deionized water, add:
2.0 g KCl   (26.9 mM)
2.0 g KH_2PO_4 (14.7 mM)
80 g NaCl   (1.37 M)
21.6 g Na_2HPO_4x$7H_2O$ (80.6 mM)

- adjust the volume to 1000 ml with deionized water

SDS sample buffer (100 ml of 4X stock)
- to 10 ml of deionized water, add:

3.0 g TRIS	(250 mM)
40 ml glycerol	(40%)
9.2 g SDS	(9.2%)
400 µg bromophenol blue	(0.4%)

- adjust the volume to 100 ml with deionized water
- prior to use add 2-ME to 10 %   (10%)

SDS running buffer (2000 ml of 10X stock)
- to 1500 ml of deionized water, add:

60.6 g TRIS	(250 mM)
288.0 g glycine	(14.4%)
20.0 g SDS	(1%)

- adjust the volume to 2000 ml with deionized water

SDS transfer buffer (2000 ml of 10X stock)
- to 1500 ml of deionized water, add:

60.6 g TRIS	(250 mM)
288.0 g Glycine	(14.4%)

- adjust the volume to 2000 ml with deionized water

TAE (1000 ml of 50X stock)
- to 500 ml deionized water, add:

242 g TRIS	(2 M)
51.1 ml acetic acid	(5.11%)
18.6 g EDTA	(500 mM)

- adjust the volume to 1000 ml with deionized water

TBS (4000 ml of 10X stock)
- to 3000 ml deionized water, add:

242 g TRIS	(500 mM)
350.65 g NaCl	(1.5 M)

- adjust the volume to 4000 ml with deionized water
- adjust to pH 7.4 if necessary

TE (509 ml)
- to 500 ml deionized water, add:

1 ml 0.5 M EDTA of pH=8.0	(1 mM)
8 ml 1 M TRIS HCL at pH=7.4	(20 mM)

- adjust to pH 7.5 if necessary

Stacking gel buffer (500 ml)
- to 350 ml of deionized water, add:

30.3 g TRIS	(0.5 M)
2.0 g SDS	(0,4%)

- adjust to pH 6.8 with concentrated HCl

- adjust the volume to 500 ml with deionized water

2.3.2   Media and gels

1%-Agarose gel (100 ml)
to 100 ml of deionized water, add:
1 g agarose (1%)
- heat to 100°C
- adjust the volume to 100 ml with deionized water
- add 20 μl/100 ml ethidium bromide
- cast gel in gel tray
- allow gel to polymerize

2%-Agarose gel (100 ml)
to 100 ml of deionized water, add:
2 g agarose (1%)
- heat to 100°C
- adjust the volume to 100 ml with deionized water
- add 20 μl/100 ml ethidium bromide
- cast gel in gel tray
- allow gel to polymerise

LB-ampicillin liquid medium (1000 ml)
- prepare LB liquid medium as described
- place stir bar into flask before autoclaving
- sterilize by autoclaving (20 min, 15 lb/sq)
- allow solution to cool to 60°C
- add 50 μg/ml ampicillin
- stir for 5 min

LB-ampicillin plates (approx. 1000 ml or 20-25 plates)
- prepare LB plates as described
- place stir bar into flask before autoclaving
- sterilize by autoclaving (20 min, 15 lb/sq)
- allow solution to cool to 60°C
- add 50 μg/ml ampicillin
- stir for 5 min
- cast into 100 mm Falcon culture dishes (20-25 ml each)

LB plates (approx. 1000 ml or 20-25 plates)
- to 900 ml of deionized water, add:
10 g Bacto tryptone
5 g Bacto yeast extract
10 g NaCl
- adjust the volume to 1000 ml with deionized water
- add 20 g Bacto agar and place stir bar into flask
- sterilize by autoclaving (20 min, 15 lb/sq)
- allow solution to cool to 60°C

- cast into 100 mm Falcon culture dishes (20-25 ml each)

Luria broth (LB) liquid medium (1000 ml)
- to 950 ml of deionized water, add:
10 g Bacto tryptone
5 g Bacto yeast extract
10 g NaCl
- adjust to pH 7.0 with 5 N NaOH
- adjust the volume to 1000 ml with deionized water
- sterilize by autoclaving (20 min, 15 lb/sq)

10% SDS-PAGE gel
- to 13 ml of deionized water, add:
8 ml resolving gel buffer
11 ml of 30% acrylamide
50 μl APS
25 μl TEMED
- cast gel between glass plates
- when gel has polymerized, prepare:
stacking gel
- to 3 ml of deionized water, add:
1.3 ml stacking gel buffer
0.8 ml of 30% acrylamide
15 μl APS
5 μl TEMED
- cast stacking gel on top of polymerised 10% SDS-PAGE gel

Terrific broth (TB) liquid medium (1000 ml)
- to 900 ml of deionized water, add:
12 g Bacto tryptone
24 g Bacto yeast extract
4 ml glycerol
- sterilize by autoclaving (20 min, 15 lb/sq)
- allow solution to cool to 60°C
- adjust the volume to 900 ml with sterile deionized water
- add 100 ml of a sterile solution of 0.17 M KH_2PO_4 and 0.72 m K_2HPO_4

2.4　Experimental procedures

2.4.1　Cell culture, γ-irradiation, and UV irradiation

Cells from the human chronic myelogenous leukemia cell-line K562 (Lozzio and Lozzio, 1977) were cultured in RPMI-1640 medium supplemented with 10% fetal calf serum (FCS) and 2 mM L-glutamine under 5.5% CO_2 at 37°C in a tissue culture incubator. Cultures were maintained in exponential growth phase (0.5×10^6 cells/ml). Cell counts were carried out using an automated cell counter. Keratinocytes were isolated from human foreskin specimens. Primary cultures were maintained in a replicative state with complete MCDB 153 medium. Secondary cultures were plated ($1\text{-}10 \times 10^3$ cells per cm^2) and medium was supplemented with 0.2% bovine pituitary extract (BPE), 0.1 mM calcium, 10 ng/ml EGF, 5 µg/ml insulin, 5×10^{-7} M hydrocortisone 1×10^{-4} M ethanolamine, and 1×10^{-4} M phosphoethanolamine. Keratinocytes were then grown to confluence in standard medium for 48 hrs. Cells were γ-irradiated as indicated at a dose rate of 11.4 Gy/min using a ^{137}Cs γ-irradiator. UV irradiation was performed using a FS20 UVB lamp in combination with a WG-295 long pass UVC filter. Quantification of the emitted doses were regularly performed using the IL 443 UVB radiometer combined with a SEE 240 photodetector.

2.4.2　Cloning and epitope-tagging

2.4.2.1　pcDNA3-AU1-*hRAD9* and pcDNA3-GFP-*hRAD9*

The *hRad9* cDNA was amplified by PCR ("touchdown-PCR") from a PCR-ready human testes cDNA library using the oligonucleotide primer pair 5'-ATG AAG TGC CTG GTC ACG GGC GGC AAC GTG AAG-3' and 5'-TCA GCC TTC ACC CTC ACT GTC TTC GCC CAG CAC-3'. The PCR products were then re-amplified using the oligonucleotide 5' primer 5'-CAG CTG CAG AGG CGC GCC AAG TGC CTG GTC ACG GGC GGC-3' that removed the initiating Met codon (5'-ATG-3') and appended an *Asc* I restriction enzyme site (5'-GGC GCG CC-3') 5' of the second codon in *hRad9*. The *Asc* I site was added to provide an in-frame fusion with either tandem AU1 epitope tags or green fluorescent protein (GFP). The 3' primer 5'-CGC CTC GAG TCT AGA TCA GCC TTC ACC CTC ACT GTC-3' added an *Xba* I site (5'-TCT AGA-3') immediately after *hRad9*'s stop codon (5'-TGA-3').

The resulting PCR fragment was digested with *Asc* I and *Xba* I and cloned into *Asc* I- and *Xba* I-digested pcDNA3 that had been pre-engineered to contain a 5' GFP or AU1 epitope tag.

2.4.2.2 pcDNA3-FLAG^2-*hRAD1*

To prepare the *hRad1* mammalian expression vector, its cDNA was PCR-amplified using the primers 5'-ATG CCC CTT CTG ACC CAA CAG ATC-3' and 5'-TCA AGA CTC AGA TTC AGG AAC TTC-3'. The amplified fragment was then re-amplified with the 5' primer 5'-GCA GGT ACC GAA TTC GCC GCC ATG GAC TAC AAA GAC GAT GAC GAC AAG GGA GAT TAC AAG GAT GAC GAT GAC AAA GGA GCC GGC GCT GGC GCG CCT CCC CTT CTG ACC-3' that incorporated an *Eco*R I site (5'-GAA TTC-3'), and a tandem FLAG epitope tag (5'-ATG GAC TAC AAA GAC GAT GAC GAC AAG GGA GAT TAC AAG GAT GAC GAT GAC AAA-3') fused in-frame with *hRad1*. Immediately upstream of the first codon of the tandem FLAG epitope tag, a Kozak consensus sequence (5'-GCC GCC-3') was incorporated. The 3' primer 5'-CTG TCT AGA CTC GAG TCA AGC CTC AGA TTC AGG AAC TTC-3' added an *Xho* I site (5'- CTC GAG-3') after *hRad1*'s stop codon. The resulting PCR fragment was digested with *Eco*R I and *Xho* I and cloned into *Eco*R I- and *Xho* I-digested pcDNA3 to yield pcDNA3-FLAG^2-*hRad1*.

2.4.2.3 pEF-BOS-ΔRI-HA^2-*hHUS1*

The *hHUS1* mammalian expression vector was prepared by amplifying *hHUS1* using the primers 5'-ATG AAG TTT CGG GCC AAG ATC CTG-3' and 5'-GGA CAG TGC AGG GAT GAA ATA CTG-3'. The resulting PCR fragment was then re-amplified with the 5' primer 5'-CAG GGT ACC GAA TTC GCC GCC ATG AAG TTT CGG GCC AAG ATC GTG-3' that added an *Eco*R I site and Kozak consensus sequence immediately upstream of the initiating Met codon. The 3' primer 5'-CAG CTC GAG TGG CGC GCC GGA CAG TGC AGG GAT GAA ATA CTG-3' removed the native stop codon, and appended an *Asc* I site (5'-GGC GCG CC-3'). The *Asc* I site provided an in-frame fusion with a tandem HA epitope tag that was pre-engineered into pEF-BOS-ΔRI. The PCR-derived DNA fragment was digested with *Eco*R I and *Asc* I and cloned into the *Eco*R I and *Asc* I sites of the HA-modified pEF-BOS-ΔRI.

2.4.3 DNA quantification

To determine DNA concentration, solution was diluted 1:25 in TE, and optical density (OD reading) was determined photometrically at wavelength λ=260 nm.

2.4.4 Amplification of DNA by polymerase chain reaction

2.4.4.1 Standard procedure

All polymerase chain reaction (PCR) amplifications were performed with the Expand high fidelity PCR system using the buffer provided by the company. A standardized setup was applied for all PCR reactions: the template mixture was prepared by mixing 2 µl of the 5'-primer and 3'-primer, both at 10 µM, 5 µl of DNA template (100 ng/ml) and 5 µl of dNTP (2 mM each) to 34 µl of sterile deionized water and placed on ice. The Master Mix (10 µl of 10X PCR buffer, 39 µl of sterile distilled water and 1 µl of Expand high fidelity polymerase) was prepared freshly. The template mixture was now placed on the heating block of the PCR thermocycler, which was preset to 94°C. The Master Mix was mixed to template mixture to a total reaction volume of 100 µl, and the thermocycler was started. For all common PCR amplifications, 30 cycles were performed with the denaturing temperature held at 94°C for 10 sec, the annealing temperature at 62°C for 30 sec and the synthesizing temperature at 72°C for 4 min.

2.4.4.2 "Touchdown-PCR"

Only amplifications of DNA from the cDNA library were performed using a "touchdown-PCR" protocol. Here, during the first 5 cycles, the denaturing temperature was held at 94°C for 10 sec and then cooled to 72°C, where the temperature was held for 3 min. During the following 5 cycles the temperature was held at 94°C for 10 sec and then ramped down to 70°C where it remained for 3 min. For the final 25 cycles the PCR machine denatured at 94°C for 10 sec, then ramped down to the annealing temperature of 64°C, which it held for 30 sec and then ramped up to the synthesis temperature of 70°C for 3 min.

2.4.5   Agarose gel electrophoresis

Agarose gel electrophoresis was used to either check the outcome of PCR amplifications, to analyze newly generated plasmids, or to gel-purify restriction enzyme digestions. According to the size of DNA fragments, the agarose gel was cast at 1% [for fragments larger than 500 base pairs (bp)], or at 2% (for fragments smaller than 500 bp). DNA products were mixed with 5X agarose gel loading buffer and separated at 100 V for 60 min. A Polaroid MP 4+ Gel Camera was used to take a Polaroid picture during UV transillumination of agarose gels to document and analyze the results of the electrophoresis. For agarose gel purification of DNA, appropriate bands were quickly cut out of the gel and purified using the Qiagen QIAquick gel extraction kit.

2.4.6   Restriction enzyme digestions

Restriction enzyme digestions were performed using the appropriate enzymes and the provided buffer purchased from New England Biolabs. For double-digestions of PCR products with two different restriction sites on the 5' and the 3'-end, respectively, 30 µl of PCR products were mixed with 5 µl of 10X reaction buffer, 11 µl of distilled water and 2 µl of each enzyme (20 units) to a total reaction volume of 50 µl. The reaction was incubated for 2 hrs at 37°C, and the reaction products were agarose gel purified. For double digestions of expression vectors, digestion was performed as described above, except the amount of DNA was limited to 5 µg, and the reaction mix was adjusted with distilled water.

2.4.7   Ligations

Ligations were performed to clone a PCR-amplified gene into a mammalian expression vector using T4 DNA ligase and the provided buffer purchased from New England Biolabs. 2 µl of 10X-reaction buffer were mixed with 1 µl of gel-purified expression vector (approximately 5 µg/ml), 2 µl of gel-purified PCR products (approximately 10 µg/µl), 16 µl of distilled water and 1 µl of T4 DNA ligase (20000 U/ml) to a total reaction volume of 20 µl. The reaction was incubated for 12 hrs at 16°C. The resulting "ligation-mix" was then used to transform competent bacteria as described below.

2.4.8 Transformations

To amplify the amount of plasmid DNA the competent Escherichia coli strain DH5α was transformed using a heat-shock protocol. 500 μl of DH5α were incubated on ice with 1-2 μl of "ligation-mix" for 30 min. Then, the cells were heat-shocked in a 42°C waterbath for 40 sec and cultured in 600 μl of LB for 1 hr. All bacterial cultures were grown with shaking (300 rpm) at 37°C in an orbital shaker. Because the plasmids confer ampicillin resistance, bacterial cells were plated on LB-amp plates to select for transformed cells and incubated overnight at 37°C.

2.4.9 DNA mini-preparation

Selected transformants were picked from overnight culture, and grown in an expansion culture of 2 ml LB for 5-8 hrs at 300 rpm in the orbital shaker at 37°C. At this step 500 μl of cell culture was saved as a glycerol stock (add 500 μl glycerol to 500 μl of bacteria cell suspension and freeze to -70°C) for use in CsCl preparations (see below). Plasmids were extracted using the Qiagen plasmid extraction kit following manufacturer's instructions. Extracted plasmid clones were then digested with restriction enzymes and analyzed by agarose gel electrophoresis (1% gel). A polaroid picture was taken to analyze the size of the fragments. All plasmids consisting of the right size fragments of vector and insert were selected for automated sequencing and those bearing no mutations were selected for cesium chloride preparation.

2.4.10 Cesium chloride DNA preparation

To obtain sufficient amounts of plasmid to carry out transient cell transfections, cesium chloride preparations were performed for each expression vector. Plasmid-containing transformants from glycerol stocks (see DNA mini-preparation) were streaked to single colonies on LB dishes containing the appropriate antibiotic (100 μg/ml ampicillin or 30 μg/ml kanamycin) required to select for plasmid and incubated at 37°C until colonies were of 1-2 mm in diameter. A single colony was picked, and transferred to a sterile 50 ml Falcon tube containing 10 ml of liquid LB-antibiotic. Bacteria-cell suspension was incubated for 8 hrs in the

orbital shaker. All incubations were carried out under vigorous shaking (300 rpm) and at 37°C. Subsequently, 1.25 ml of start-up culture were transferred to a sterile 1000 ml Erlenmeyer flask. 125 ml of antibiotic containing Terrific Broth (TB-antibiotic) were added, and the suspension was incubated for 12-14 hrs. Then, cells were transferred to 250 ml Nalgene centrifuge tube and centrifuged at 3700 rpm for 20 min. The cell pellet was re-suspended in 16 ml of freshly prepared GTE buffer and added to a sterile 250 ml beaker. After 10 min of incubation with 2 ml of lysozyme solution at 37°C, cells were lysed for 5 min by addition of 32 ml of NaOH/SDS buffer. Thereafter, to precipitate the SDS protein complexes, 26 ml of KAc solution were added to cell lysates, and the solution was shaken, and incubated on ice for 15 min. To separate DNA from cell debris, the solution was centrifuged in a Beckman J2-21 centrifuge equipped with a JA-17 rotor at 17000 rpm (40000xg) for 20 min at 4°C. The supernatant was filtered through a fine mesh and precipitated by addition of 2 volumes of 100% ethanol. To collect the precipitated DNA, solution was centrifuged for 20 min at 3000 rpm at 4°C, the supernatant was discarded carefully, and the DNA pellet was air-dried to remove the residual ethanol. The dry pellet was dissolved in 16 ml TE. To separate plasmid DNA from chromosomal DNA, a cesium-chloride (CsCl) gradient (1 g/ml) was induced by addition of 20 g of CsCl to dissolved DNA. Additionally, 0.45 ml of ethidium bromide (10 mg/ml) and 0.45 ml of sarcosyl were added. The solution was then filled into two 11.2 ml OptiSeal ultracentrifuge tubes and centrifuged at 60000 rpm (~371000xg) at 25°C for 8 hrs using a Beckman L8-70 Ultra Centrifuge equipped with a NVT 65 rotor. The plasmid-containing band (lower pink band) was removed using a sterile syringe and needle. The volume (V) was measured, and TE was added to a total of 17.2 ml. To create the second CsCl gradient, [19.8 g - (V) g] CsCl and 0.4 ml ethidium bromide were added. Gradients were centrifuged for 8 hrs (60000 K, 25°C). The plasmid-containing bands were aspirated with a sterile syringe and needle. To remove the ethidium bromide, the volume was adjusted to 5 ml with TE. 15 ml of 95% ethanol were added to precipitate DNA. Centrifugation in the Beckman J2-21 centrifuge equipped with a JA-17 rotor at 7000 rpm (10000xg) provided a DNA pellet that was again dissolved in 5 ml TE. This step was repeated until DNA was no longer pink, which indicated that it was clear of ethidium bromide. The final precipitate was dissolved in 5 ml TE, and the concentration of DNA was determined photometrically at wavelength $\lambda=260$ nm.

2.4.11   Transient transfections

To transiently express a gene of interest in K562 cells, the expression vector was introduced into the cell by electroporation. All electroporations (transfections) used 40 µg of plasmid DNA, which included empty vector added to this amount, if necessary. For precipitation, DNA was aliquotted into an Eppendorf tube, and TE buffer was added to 300 µl. After addition of 30 µl of 3 M sodium acetate and 600 µl of 95% ethanol, the tube was shaken thoroughly and subsequently centrifuged for 5 min at 20000xg. The supernatant was carefully aspirated, and an additional 1 ml of 95% ethanol was added to wash the DNA pellet. After centrifugation for 30 sec at 20000xg, all traces of ethanol were vacuum-aspirated using a sterile needle under the tissue culture hood. The DNA precipitate was then dissolved for 20 min in 50 µl RPMI 1640 medium without FCS and L-glutamine with occasional vortexing. For each transfection, 1×10^7 K562 cells in exponential growth phase were pelleted by centrifuging (800xg), and all traces of medium were aspirated. The cells were re-suspended in 350 µl RPMI-1640 medium (with 10% FCS and L-glutamine) and incubated with dissolved DNA (50 µl) in a total volume of 400 µl. After 5 min, the cell-DNA mixture was transferred to a 4 mm BTX electroporation cuvette. A BTX T 820 electroporator was used to deliver a 344-volt, 10-msec pulse. Electroporated cells were plated on 100 mm Falcon culture dishes in FCS/L-glutamine-containing RPMI-1640 medium and cultured for 16-24 hrs before use in experiments. The construction, operation and efficiency of the electroporation apparatus have been described (Fakhrai et al., 1996; Takahashi et al., 1991)

2.4.12   Co-immunoprecipitation experiments

Exponentially growing K562 cells were either transfected as indicated above or used directly for immunoprecipitation studies. Cells were centrifuged for 5 min (800xg), washed in PBS, and lysed in lysis buffer. The cell lysates were then immunoprecipitated with the indicated mouse monoclonal antibodies and protein G-Sepharose or rabbit antisera and protein A-Sepharose for 1 hr at 4°C. The immunoprecipitates were washed three times with lysis buffer, heated to 100°C for 5 min in 1X-SDS-PAGE sample buffer, and fractionated in 10% gels by sodium dodecylsulfate-polyacrylamide gel electrophoresis (SDS-PAGE). A Hoefer SE 600 series Electrophoresis Unit in combination with a Power Pac 1000 power supply was used to

run the gels. The gels were transferred to Immobilon P membranes. For transfer runs, a Hoefer TE series Transphor Electrophoresis Unit in combination with a Power Pac 200 was used. Subsequently, the membranes were blocked in 5% bovine serum albumin (BSA) in TBS containing 0.2% Tween 20, and immunoblotted with the indicated antibodies or antisera in TBS containing 0.2% Tween 20 and 5% BSA. hRad9, hHus1, and hRad1 rabbit antisera were diluted 1:500 while the monoclonal mouse antibodies (mAB) were diluted 1:5,000. For immunoblots with the mAB, the membranes were washed and then incubated with rabbit anti-mouse IgG conjugated to horseradish peroxidase (1:5,000 dilution) or rabbit anti-mouse IgG in TBS containing 0.2% Tween 20 (1:5,000 dilution), followed by incubation with horseradish peroxidase-conjugated protein A (1:10,000 dilution). For immunoblots with rabbit antisera, after incubation in the primary rabbit antibody solutions, the blots were washed and then incubated with horseradish peroxidase-conjugated protein A (1:10,000 dilution). All membranes were developed with SuperSignal chemiluminescent substrate.

2.4.13 Sequential blotting

For membranes that were sequentially blotted with different antisera, the membranes were stripped of bound antibodies with two 30-minute washes of 8 M guanidine hydrochloride, prior to blocking and immunoblotting.

2.4.14 Mobility shift experiments

Exponentially growing K562 cells (1×10^7 per assay point) were treated with the indicated stimuli and cultured as described. The cells were then centrifuged (800xg, 5 min), washed with PBS, and lysed in lysis buffer. The lysates were clarified by centrifugation for 5 min at 21,000xg in a table top centrifuge at 4°C and rotated with 5 µl anti-hRad9 antiserum on protein A-Sepharose for 1 hr. The immunoprecipitates were washed three times with lysis buffer, heated at 100°C for 5 min in 1X SDS-PAGE sample buffer, and fractionated by SDS-PAGE (10% gel). The gels were transferred to an Immobilon-P membrane, and the membranes were immunoblotted with a 1:500 dilution of anti-hRad9 antiserum in TBS containing 0.2% Tween 20. The antigen-antibody complexes were detected with a 1:10,000 dilution of horseradish peroxidase-conjugated protein A.

2.4.15   Phosphatase experiments

Exponentially growing K562 cells (1×10^7 per sample) were treated with 0 or 50 Gy IR and cultured for 5 hrs at 37°C. The cells were then lysed, and hRad9 was immunoprecipitated as described above. The immunoprecipitates were washed three times with lysis buffer and three times with 50 mM TRIS, pH 8.5, 0.1 mM EDTA. Samples that were not treated with phosphatase were then mixed with SDS-PAGE sample buffer. Samples treated with phosphatase were incubated with 0.25 units of calf intestinal phosphatase for 30 min at 30°C, with or without 50 mM β-glycerophosphate, following manufacturer's directions (Gibco BRL, Gaithersburg, MD). After phosphatase treatment, the immunoprecipitates were washed once with lysis buffer, mixed with SDS-PAGE sample buffer, and fractionated by SDS-PAGE (10% gel).

2.4.16   *In vitro* translations

These were performed with the TnT Quick Coupled Transcription/Translation System using pcDNA3-FLAG^2-*hRAD1* and pcDNA3-*hHUS1*-HA^2 as templates for the reactions. A portion (10 μl) of each translation reaction was prepared for SDS-PAGE. The remainder of each was divided into two parts. Each part (20 μl) was diluted into 1 ml of lysis buffer and was immunoprecipitated with either anti-FLAG mAb or anti-HA mAb and protein G-Sepharose, and fractionated by SDS-PAGE (10% gel).

2.4.17   Antibodies

Bacterial expression vectors for hexahistidine-tagged hRad1 and hHus1 were generated by cloning PCR-amplified DNA fragments into pET24a+. Histidine-tagged proteins were induced and purified according to manufacturer's instructions. PCR-derived DNA fragments for hRad9 were cloned into pGEX-KG to generate an in-frame fusion with glutathione S-transferase (GST). Bacterially produced GST-hRad9 was purified by affinity chromatography on glutathione agarose (GSH). The purified proteins were used to immunize rabbits to generate antisera against hRad9, hHus1, and hRad1. The anti-GFP rabbit antiserum was obtained from Molecular Probes (Eugene, OR). The anti-HA and anti-AU1 monoclonal

antibodies were purchased from Babco (Berkeley, CA), and the anti-FLAG mAb was from Kodak (New Haven, CT).

2.4.18 Fluorescent microscopy

To explore a proteins localization within the cell, the protein was epitope-tagged with enhanced green fluorescent protein (GFP). GFP is a monomeric protein of 27 kDa (238 amino acids). It autocatalytically forms a fluorescent pigment that emits green light in response to excitation (maximally at 488 nm) in the absence of any co-factors. GFP may therefore be used as a fluorescent tag to monitor protein localization. (Chalfie et al., 1994). Exponentially growing K562 cells (5×10^6 per sample) were transfected with 5 µg GFP-tagged hRad9, 5 µg GFP-N1 alone and empty vector as described. Approximately 15000 cells were spun down on a coverslip using a cytospin centrifuge. Cells were fixed on coverslips with 4% paraformaldehyde in PBS for 3 min, and subsequently, nuclei were counter-stained for 3 min with 10 µg/ml propidium iodide in PBS (red fluorescence in response to excitation). Coverslips were air-dried and mounted on microscope slides with Vectashield Antifade Mounting Medium. Coverslips were sealed with clear nail polish. Fluorescent microscopy was performed at a wavelength of 488 nm using the Confocal Laser Scanning Microscope LSM510. Images were created with the LSM510 software for windows NT and saved as TIFF files.

3 Results

3.1 Human checkpoint proteins hRad9, hHus1, and hRad1 associate in a complex

Comparisons of the predicted protein sequences of the human proteins analyzed in this study (hRad9, hHus1, and hRad1) to their putative homologs in the fission yeast *S. pombe* reveal homologies widely extending over large portions of each protein. The human proteins are 25-30% identical and 52-57% similar to their respective homologs at the amino acid level (Udell et al., 1998; Savitsky et al., 1995; Lieberman et al., 1996; Parker et al., 1998; Kostrub et al., 1998; Sanchez et al., 1997; Freire et al., 1998). In wild-type fission yeast (*S. pombe*), the checkpoint proteins spRad1 and spHus1 interact genetically as well as physically, demonstrating that checkpoint proteins form biochemical complexes. This interaction does not occur in yeast with mutant spRad9, suggesting that spRad9 is required for hHus1-hRad1 interaction. One interpretation of this result is that spRad9 may physically link spRad1 to spHus1, although this hypothesis has not been validated experimentally (Kostrub et al., 1998).

To address whether structural organization of the checkpoint protein complexes are conserved from yeast to humans, we examined the ability of the human homologs of spRad9, spHus1, and spRad1 to form biochemical complexes similar to those reported in yeast. Using polyclonal rabbit antibodies of hRad9, hHus1, and hRad1 we immunoprecipitated each protein from detergent cell lysates of exponentially growing K562 cells. The precipitates were then separated by SDS-PAGE, transferred to a membrane, and sequentially immunoblotted with antibodies that recognize the potential interaction partners.

Human K562 cell lysates that were immunoprecipitated with anti-hHus1 antiserum (Fig. 1A, left panel) contained a protein band of 34 kilodalton (kDa), which was similar in size to hHus1's predicted molecular weight of 32 kDa. The hHus1 immunoprecipitates also contained a 33-kDa band, which reacted with the anti-hRad1 antiserum (Fig. 1B, left panel). This band co-migrated with immunoprecipitated hRad1 and corresponded in size to hRad1's predicted mass of 31 kDa, suggesting that hRad1 physically binds to hHus1 *in vivo*. Immunoblotting of the hHus1 immunoprecipitates with anti-hRad9 antiserum revealed a 70-kDa band (Fig. 1C, left panel) that co-migrated with a band in the anti-hRad9 precipitates (Fig.

1C, right panel). This was surprising, as hRad9 has a predicted molecular mass of 45 kDa, which is much smaller than the 70-kDa band observed. As will be shown, the hRad9 protein undergoes extensive post-translational modification (Fig. 2, 3), which likely accounts for the discrepancy between its apparent and predicted molecular masses. We therefore conclude that hRad9, as well as hRad1, physically binds to hHus1 *in vivo*.
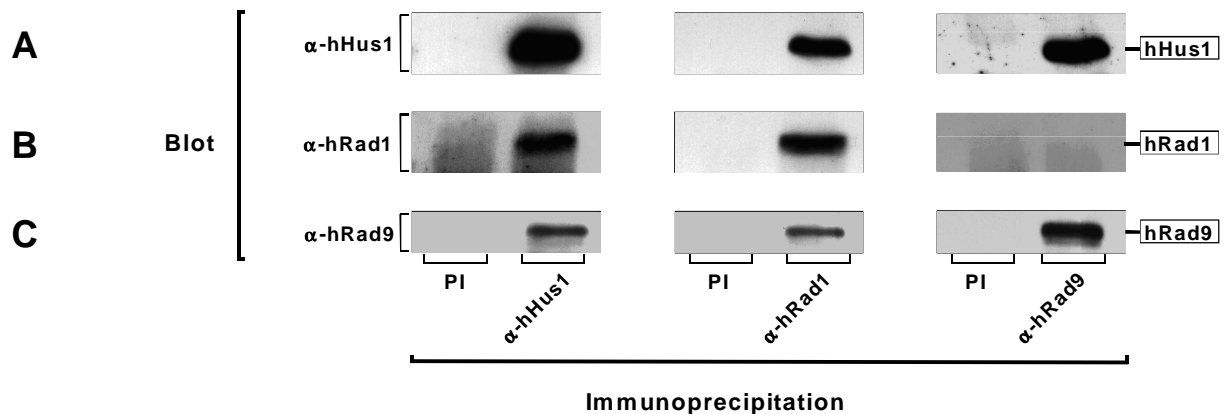

Figure 1. hRad9, hHus1, and hRad1 associate in a stable complex. **(A)** Lysates prepared from exponentially growing K562 cell (1×10^7 per sample) lysates were immunoprecipitated with either preimmune (PI) antisera or with anti-hRad9, anti-hRad1, or anti-hHus1 rabbit antisera. After extensive washing, the immunoprecipitates were fractionated by SDS-PAGE (10% gel), transferred to Immobilon P, and immunoblotted with hRad9, hHus1, or hRad1.

To further verify that these proteins associate, we immunoprecipitated hRad9 in K562 cell lysates. In these precipitates we readily observed a hHus1-reactive band (Fig. 1A, right panel) that co-migrated with immunoprecipitated hHus1 (Fig. 1A, left panel). We also immunoprecipitated hRad1 and demonstrated that hHus1 (Fig. 1A, middle panel) was present in anti-hRad1 immunoprecipitates. However, we did not detect hRad1 protein in hRad9 immunoprecipitates (Fig. 1B, right panel), even though we did observe hRad9 in anti-hRad1 immunoprecipitates (Fig. 1C, middle panel). A possible explanation for these discrepant results is that hRad1 and the immunodominant anti-hRad9 antibodies share an overlapping binding site, which precludes simultaneous interaction. Alternatively, antibody binding to hRad9 induces conformational changes of hRad9 that inhibit interaction of hRad1 and hRad9. In support of this, Figure 4 demonstrates that anti-AU1 immunoprecipitates of AU1-tagged hRad9 do contain hRad1. These results suggest that this group of human checkpoint proteins

as well as their yeast counterparts assembles into multimolecular complexes, even in the absence of genotoxic stimuli.

3.2 hRad9 undergoes complex post-translational modifications

To generate a model system of checkpoint protein function amenable to biochemical analysis, we prepared epitope-tagged expression vectors for hRad9, hHus1, and hRad1. The cDNAs were obtained by PCR amplification from a human testes cDNA library using primers containing the sequence of the respective epitope. In this way, we generated hRad1 linked to a tandem FLAG-epitope (hRad1-FLAG^2), hHus1 linked to two HA-epitopes (hHus1-HA^2), and hRad9 linked to either an AU1-epitope (hRad9-AU1) or to GFP (hRad9-GFP). These expression vectors were transfected into K562 cells by electroporation, which resulted in transient expression of epitope-tagged protein within 16-24 hrs.

Immunoprecipitation studies (Fig. 1) revealed that, when analyzed by SDS-PAGE, hRad9 migrated with an apparent molecular mass that was much larger (70 kDa) than predicted (45 kDa), suggesting that the entire cellular pool of hRad9 may undergo extensive post-translational modifications. Consistent with this observation, overexpression of AU1-tagged hRad9 revealed multiple species when resolved by SDS-PAGE (Fig. 2, lane 5). The major band detectable had an apparent molecular mass of 55 kDa. This is significantly smaller than the 70-kDa endogenous hRad9 (Fig. 2, lanes 2 and 3), but still larger than the predicted molecular mass (45 kDa), even when the 2-kDa epitope tag is taken into account. Thus, the major 55-kDa may be either an unmodified form that migrates anomalously or a partially modified version. In addition to the 55-kDa form, multiple slower-migrating bands were present above this band, suggesting several steps of post-translational modification (Fig. 2, lane 5). Remarkably, co-expression of hRad9-AU1 with hHus1-HA and hRad1-FLAG resulted in a large increase of the amount of a highly modified, 72-kDa form of hRad9. This slow-migrating form of hRad9 had an apparent molecular mass slightly greater than endogenous hRad9, which is due to the addition of the tandem AU1 tag on hRad9 (Fig. 2, lane 6). Taken together, these results suggest that endogenous hRad9 is quantitatively and extensively modified. Furthermore, limiting cellular factors, possibly hRad1 and hHus1, are required for modification of hRad9.
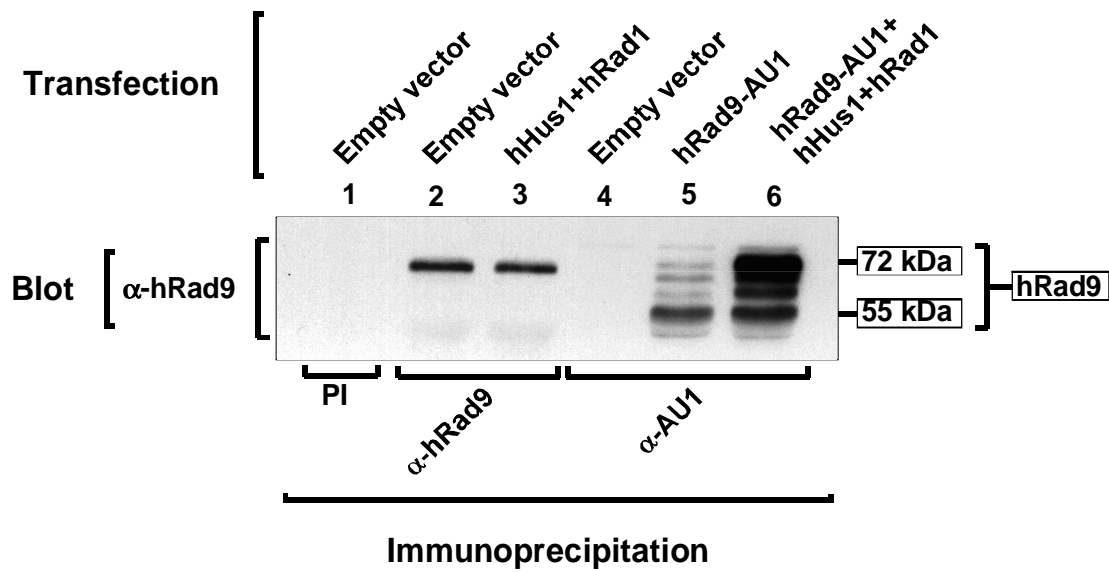
Figure 2. Transiently overexpressed hRad9 undergoes complex modifications. K562 cells (1×10^7 cells per sample) were transiently transfected with 40 μg pcDNA3 empty vector only (lanes 1, 2, and 4), with 5 μg pEF-BOS-ΔRI-hHus1-HA^2 and 5 μg pcDNA3-FLAG^2-hRad1 expression vectors (lane 3), with 20 μg AU1-hRad9 alone (lane 5), or with these amounts of pEF-BOS-ΔRI-hHus1-HA^2 together with pcDNA3-FLAG^2-hRad1 and AU1-hRad9 (lane 6). In all cases empty vector was added so that all transfections contained a total of 40 μg DNA. The following day, cell lysate were immunoprecipitated with either preimmune serum (PI, lane 1), anti-hRad9 (lanes 2 and 3), or anti-AU1 mAb (lanes 4-6). Immunoprecipitations were fractionated by SDS-PAGE (10% gel), transferred to Immobilon P and blotted with anti-hRad9. The arrows indicate apparent molecular masses of AU1-hRad9 calculated using commercially available protein standards.

3.3 Co-expression of hRad1 and hHus1 enhance accumulation of modified hRad9

As observed in Figure 2, co-expression of hRad1 and hHus1 has an obvious impact on the accumulation of modified hRad9. To further explore the role of hRad1 and hHus1 in the modification of hRad9, we transfected K562 cells with a constant amount of GFP-tagged hRad9 along with increasing amounts of the hRad1 and hHus1 expression vectors (Fig. 3). In this experiment, the protein-containing membrane was immunoblotted sequentially with anti-GFP (hRad9) antiserum (Fig. 3A), then with anti-FLAG (hRad1) antiserum (Fig. 3B), and finally with anti-HA (hHus1) antiserum (Fig. 3C). Between these sequential immunoblottings, the membrane was washed in 8 M guanidine hydrochloride solution to remove the bound antibody. Like hRad9-AU1, GFP-tagged hRad9 also undergoes extensive alterations in mobility when resolved with SDS-PAGE. In the absence of co-expressed hRad1 and hHus1 there was little conversion of hRad9 to the most highly modified form (Fig. 3A, lane 2). As expression of hRad1 and hHus1 increases (Fig. 3B and C, lanes 3-6) there is concomitant enhanced formation of the most highly modified form of hRad9 (Fig. 3A, lanes 3-6). These results, coupled with the results presented in Figure 2, demonstrate that hRad1 and hHus1 either promote formation of, or stabilize the modified form of hRad9.
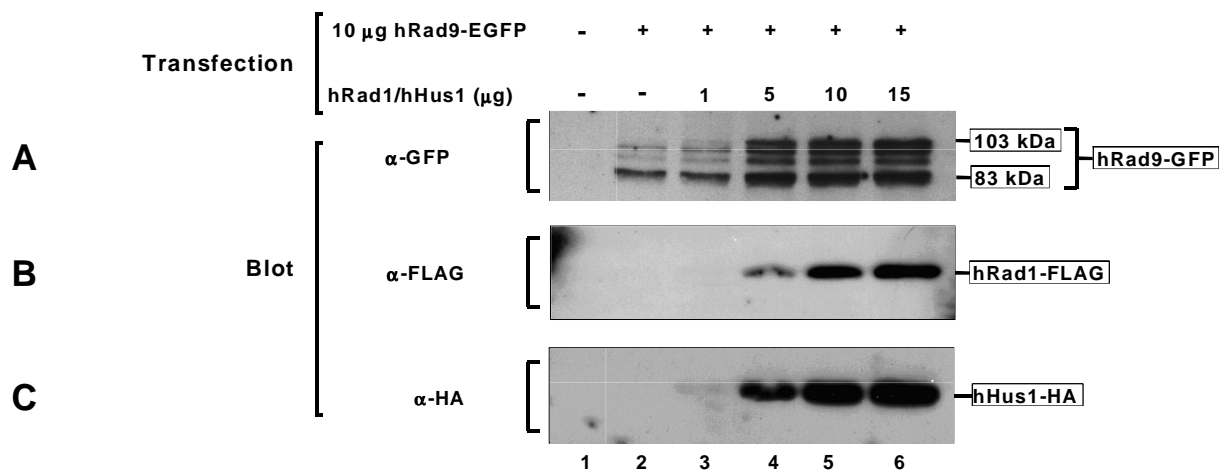
Figure 3. hRad1 and hHus1 promote the formation of slower-migrating forms of hRad9. K562 cells (1×10^7 per sample) were transfected with pcDNA3 empty vector alone (-, lane 1) or 10 μg pcDNA3-GFP-hRad9 (lanes 2-6), along with increasing amounts of pEF-BOS-ΔRI-FLAG^2-hRad1 and pcDNA3-hHus1-HA^2 (lanes 3-6). The cell lysates were then resolved by SDS-PAGE (10% gel) and immunoblotted sequentially (with stripping between) with anti-FLAG, anti-HA, and then with anti-GFP rabbit antiserum. The corresponding immunoreactive bands are indicated. The apparent molecular mass of GFP-hRad9 was estimated by comparisons with molecular weight standards.

3.4   Epitope-tagged proteins hRad9, hHus1, and hRad1 associate in a modification-dependent manner

To test whether the transiently expressed checkpoint proteins serve as a functional model system, we asked whether the epitope-tagged proteins form complexes similar to those formed by endogenous proteins. We thus tested whether hRad9-AU1, hHus1-HA, and hRad1-FLAG recapitulate complex formation of endogenous proteins as observed in Figure 1. Four sets of K562 cells were transfected with either empty expression vector alone, a combination of hRad9-AU1, hHus1-HA, and hRad1-FLAG alone, or expression vectors of all three proteins (Fig. 4, lanes 1-4, 5-8, 9-12, and 13-16). To detect endogenous hRad9 and epitope-tagged hRad9 simultaneously, we performed the immunoblots using the rabbit anti-hRad9 antiserum. Anti-hRad9 immunoblots of cell lysates (Fig. 4C, lanes 1-4) revealed that epitope-tagged hRad9 was highly overexpressed compared to the 70-kDa endogenous hRad9 (Fig. 4C, lanes 3 and 4 vs. lanes 1 and 2), which was not visible on this exposure. Consistent with the results presented in Figures 2 and 3, there were multiple forms of AU1-tagged hRad9, and co-

expression of hRad1 and hHus1 enhanced the accumulation of the highly modified form (Fig. 4C, lane 15 vs. lane 16).

To assess associations among transiently expressed proteins, we immunoprecipitated hRad1-FLAG (Fig. 4, lanes 5-8), hHus1-HA (Fig. 4, lanes 9-12), and hRad9-AU1 (Fig. 4, lanes 13-16) and blotted with antisera recognizing each of the three proteins. In hRad1 precipitates we detected epitope-tagged hRad1 (Fig. 4A, lanes 6 and 8), epitope-tagged hHus1 (Fig. 4B, lanes 10 and 12), and both endogenous hRad9 (Fig. 4C, lane 6) and epitope-tagged hRad9 (Fig. 4C, lane 8). We also immunoprecipitated hHus1-HA (Fig. 4, lanes 9-12) and found hHus1 (Fig. 4B, lanes 10 and 12), associated hRad1 (Fig. 4A, lanes 10 and 12) and hRad9 (Fig. 4C, lanes 10 and 12). Again, as observed in the hRad1 (anti-FLAG) immunoprecipitates, endogenous and AU1-tagged hRad9 were present in the complex (Fig. 4C, lanes 10 and 12). Strikingly, in both the hRad1 and hHus1 precipitations, only the most highly modified form of transfected hRad9 associated with hRad1, suggesting that the modification is essential for interaction with the checkpoint proteins hRad1 and hHus1. The effect is not specific to the AU1-tagged hRad9, as we have also observed that only highly modified GFP-hRad9 interacts with hHus1 and hRad1 (data not shown).

In the reciprocal experiment we observed that hRad1 (Fig. 4A, lane 16) and hHus1 (Fig. 4B, lane 16) co-precipitated with immunoprecipitated hRad9 (Fig. 4, lanes 13-16). Unlike our observations with the endogenous proteins, hRad1 was detected readily in the anti-hRad9-AU1 immunoprecipitations, thus strongly suggesting that our rabbit anti-hRad9 antiserum indeed masks or disrupts interaction of endogenous hRad1 and hRad9 (Fig. 1). Taken together, these results revealed that the epitope-tagged human checkpoint proteins hRad1 and hHus1 associated selectively with modified hRad9 in undamaged cells. Thus, the assembly of transiently expressed, epitope-tagged checkpoint proteins mimics the complex formation of the endogenous proteins (Fig. 1).
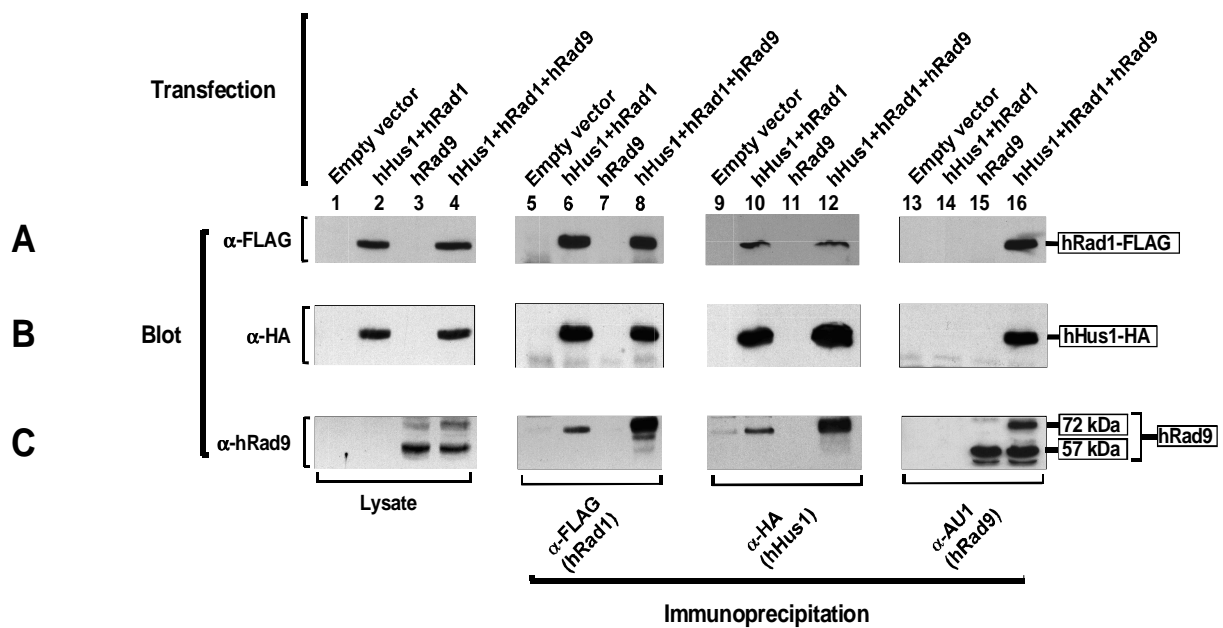
Figure 4. Transiently expressed, epitope-tagged hRad9, hHus1, and hRad1 interact. Cells (1×10^7 per sample) were transfected with 40 μg pcDNA3 (lanes 1, 5, 9, 13), 30 μg pcDNA3-AU1[2]-hRad9 (lanes 3, 4, 7, 8, 11, 12, 15, 16), 5 μg pEF-BOS-ΔRI-hHus1-HA[2] (lanes 2, 4, 6, 8, 10, 12, 14, 16) or 5 μg pCDNA3-FLAG[2]-hRad1 expression vectors. If required, the total amount of DNA (40 μg) in each transfection was kept constant by the addition of empty vector. 20 hrs after transfection, the cells were lysed, and an aliquot of each lysate was prepared for electrophoresis (lysate). The lysates were immunoprecipitated with anti-FLAG, anti-HA, or anti-AU1 mAb, and lysates and immunoprecipitates were fractionated by SDS-PAGE (10% gel) and transferred to Immobilon P. The membrane was immunoblotted sequentially with **(C)** anti-hRad9, **(A)** anti-Flag, followed by **(B)** anti-HA. Arrows indicate the positions of the labeled proteins. The apparent molecular mass of AU1-hRad9 was estimated by comparison to protein standards.

3.5 hRad1 and hHus1 interact independently of hRad9 *in vivo* and *in vitro*

Based on studies in *S. pombe*, where spRad1 and spHus1 did not associate in yeast mutants that lack spRad9, we reasoned that hRad1 and hHus1 would not interact in the absence of hRad9 (Kostrub et al., 1998). To test this idea, we overexpressed hRad1 and hHus1 together (without hRad9 overexpression) and assessed their interaction. Figure 5A demonstrates that even in the absence of overexpressed hRad9, hRad1 co-precipitated with hHus1 (Figure 5A, lower panel, lane 8), and hHus1 co-precipitated with hRad1 (Fig. 5A, upper panel, lane 12). This interaction appears to be specific since no hRad1-FLAG was detected in hHus1-HA precipitates from cells that were transfected with hHus1-HA only (Fig.

40

5A, lower panel, lane 6). Neither was hHus1-HA detected in hRad1-FLAG immunoprecipitates from cells that were not expressing hHus1-HA (Fig. 5A, upper panel, lane 11). As shown in Figure 4, endogenous hRad9 was also found in a complex with overexpressed hRad1 and hHus1, leaving open the possibility that endogenous hRad9 may mediate the interaction of the overexpressed hRad1 and hHus1. Because hRad1 and hHus1 are highly overexpressed (data not shown), these results may indicate that these proteins interact without other components of the complex. To test whether hRad9 is required for hRad1 and hHus1 interaction, we transcribed and translated both proteins *in vitro* alone or in combination (Fig. 5B). The translation mixtures were then immunoprecipitated with anti-FLAG (hRad1) or anti-HA (hHus1) antibodies and resolved by SDS-PAGE. Immunoblotting of the anti-FLAG immunoprecipitations with anti-HA showed that hHus1-HA co-precipitated with hRad1-FLAG (Fig. 5B, upper panel, lane 12). Blotting of the anti-HA immunoprecipitations with anti-FLAG revealed that hRad1-FLAG co-precipitated with hHus1-HA (Fig. 5B, lower panel, lane 8). This suggests that, unlike in yeast, these proteins associate in the absence of hRad9.
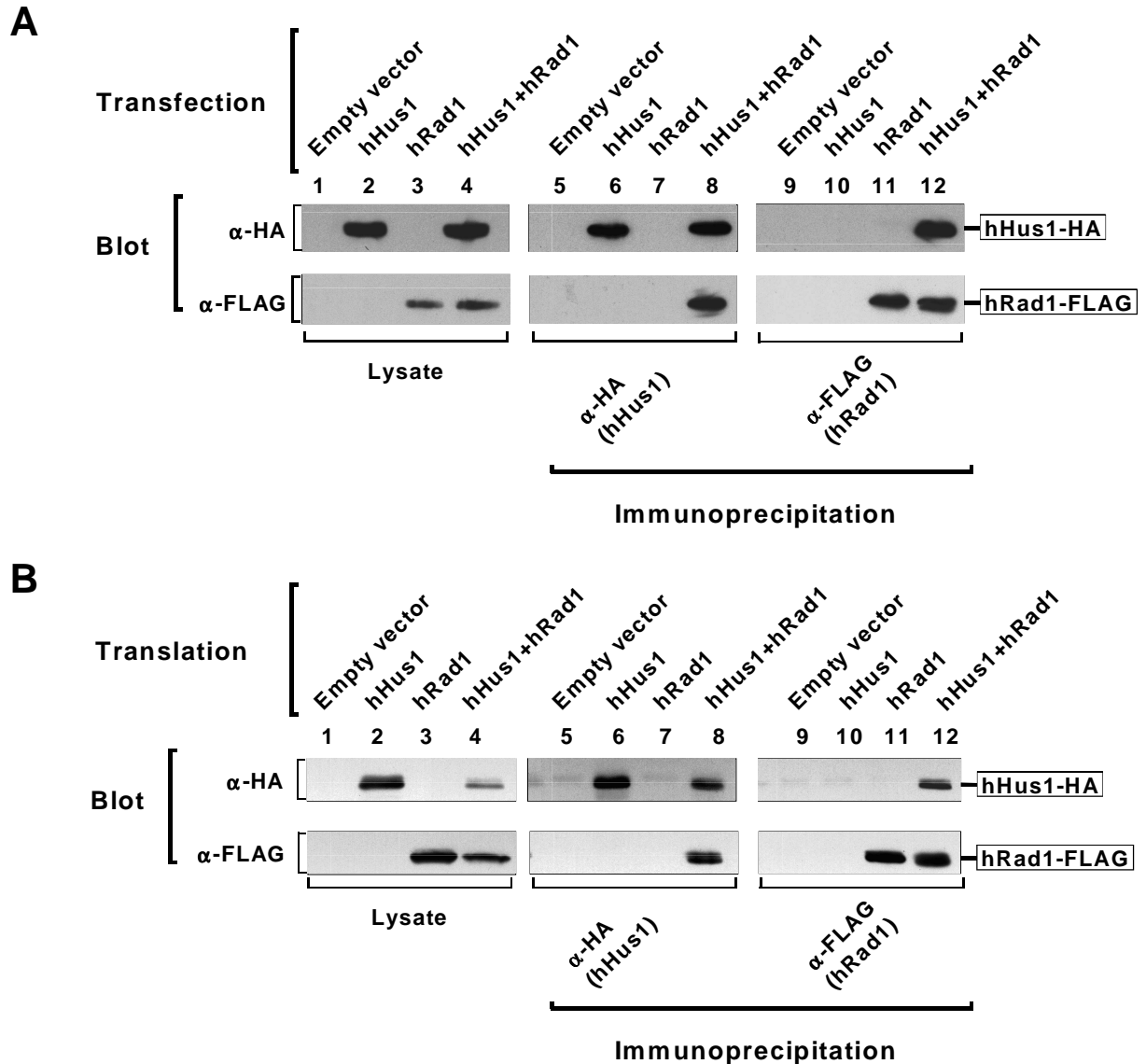
Figure 5. hRad1 and hHus1 form a stable dimeric complex. (**A**) Cells ($1x10^7$ per sample) were transfected with pcDNA3 empty vector (lanes 1, 5, 9), pEF-BOS-ΔR1-hHus1-HA^2 alone (lanes 2, 6, 10), pcDNA3-FLAG^2-hRad1 alone (lanes 3, 7, 11), or both expression vectors (lanes 4, 8, 12). Cell lysates were prepared, and a portion was prepared for analysis by SDS-PAGE. The lysates were then immunoprecipitated with anti-HA or anti-FLAG mAbs. The lysates and immunoprecipitates were then resolved by SDS-PAGE (10% gel) and immunoblotted with anti-FLAG followed by anti-HA. The migration positions of the epitope-tagged proteins are indicated. (**B**) *In vitro* transcription and translation reactions were performed with either 1 µg pcDNA3 empty vector (lanes 1, 5, and 9), 1 µg pcDNA3-hHus1-HA^2 alone (lanes 2, 6, and 10), 1 µg pcDNA3-FLAG^2-hRad1 alone (lanes 3, 7, and 11), or 1 µg of both pcDNA3-HA^2-hHus1 and pcDNA3-FLAG^2-hRad1 together (lanes 4, 8, and 12).

3.6 hRad9 does not associate with hHus1 or hRad1 alone

In *S. cerevisiae*, interaction of the checkpoint proteins scDdc1 (homolog of hRad9) and scMec3 was dependent on the presence of scRad17 (homolog of hRad1; Paciotti et al., 1998). We thus asked whether hHus1 interacted with hRad9 in the absence of overexpressed hRad1. K562 cells were transfected with empty vector alone, expression vectors for all three proteins, or with expression vectors for hRad9 and hHus1 alone. Immunoprecipitation of hHus1 revealed that hRad9 (Fig. 6A, lane 5) and hRad1 (Fig. 6B, lane 5) associated with hHus1 when all three proteins were co-expressed. In the absence of hRad1, hRad9 did not interact with hHus1 (Fig. 6A, lane 6). Correspondingly, hRad9 immunoprecipitations (anti-GFP) did not contain hHus1 (Fig. 6C, lane 9) unless hRad1 was also expressed (Fig. 6C, lane 8). We note that expression levels of hHus1 (Fig. 6C, lanes 2 and 3) are not equal. This was repeatedly observed in experiments where hRad9 and hHus1 were co-expressed in the absence of hRad1, suggesting that hHus1 accumulation is by some means dependent of hRad1 expression. In favor of this hypothesis is the observation that spHus1 levels are significantly decreased in yeast mutants lacking the *sprad1* gene (Kostrub et al., 1998).

We next asked whether hRad1 associated with hRad9 in the absence of co-expressed hHus1. Cells were transfected with empty vector only, with all three checkpoint protein expression vectors, or with hRad9 and hRad1 only (Fig. 7). In cells expressing all three proteins, both hHus1 (Fig. 7B, lane 5) and hRad9 (Fig. 7A, lane 5 and Fig. 7C, lane 8) associated with hRad1. hRad1 did not associate with hRad9 in cells transfected with only hRad1 and hRad9 (Fig. 7A, lane 6 and Fig. 7C, lane 9), even though expression levels of hRad1 and hRad9 were similar in both cases. Therefore, the results presented in Figures 6 and 7 suggest that hRad1 and hHus1 form an independent molecular complex. Furthermore they indicate that interaction of hRad9 with either hRad1 or hHus1 requires the presence of both hRad1 and hHus1.
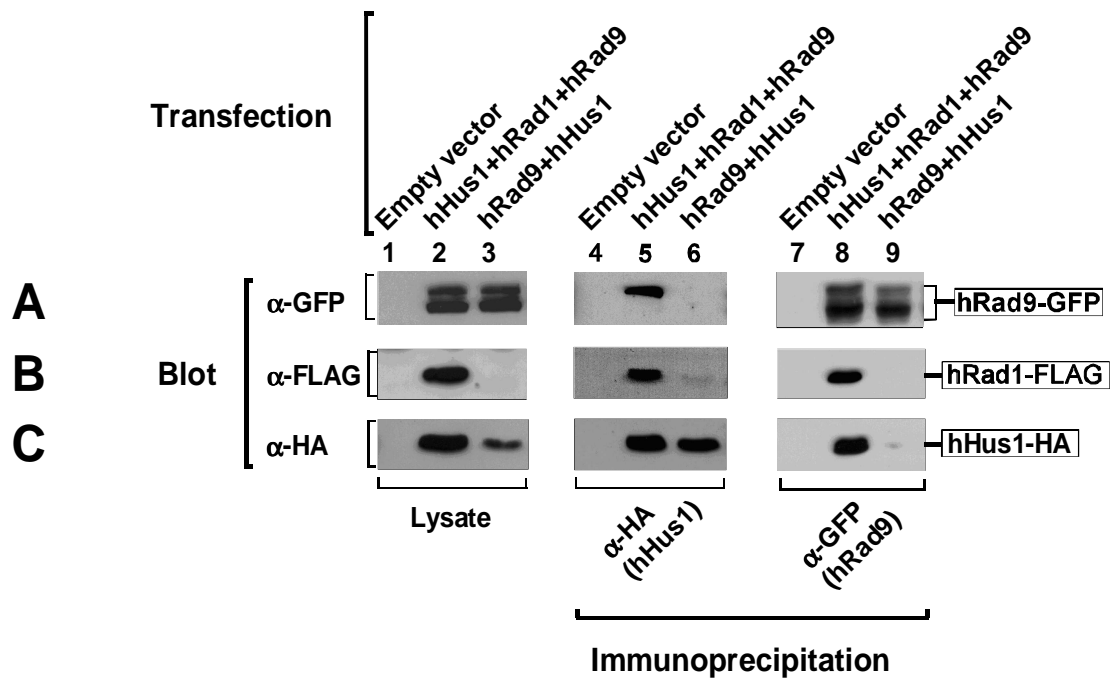
Figure 6. Transiently expressed hHus1 and hRad9 alone do not interact. K562 cells (1×10^7 per sample) were transfected with pcDNA3 empty vector (lanes 1, 4, 7), the combination of 5 μg pEF-BOS-ΔRI-HA^2-hHus1, 5 μg pcDNA3-hRad1-FLAG^2, and 30 μg pcDNA3-AU1^2-hRad9 expression vector together (lanes 2, 5, 8), or with 5 μg pEF-BOS-ΔRI-HA^2-hHus1 30 μg pcDNA3-AU1^2-hRad9 only (lanes 3, 6, 9). A portion of the lysate was prepared for SDS-PAGE, and the remainder was immunoprecipitated with anti-FLAG or anti-GFP. The cell lysates and immunoprecipitates were resolved by SDS-PAGE (10% gel), transferred to Immobilon P, and immunoblotted sequentially with **(B)** anti-FLAG and **(C)** anti-HA mAbs, followed by immunoblotting with **(A)** anti-GFP antiserum.
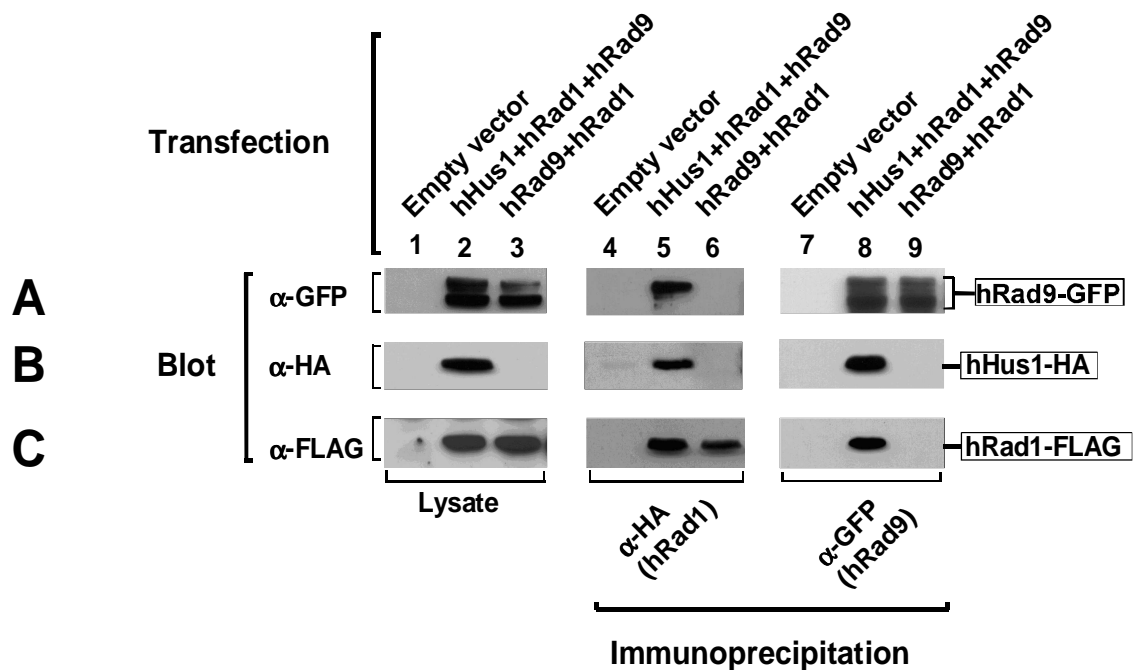
44

Figure 7. Transiently expressed hRad1 and hRad9 alone do not interact. Log-phase K562 cells (1x10^7 per sample) were transfected with pcDNA3 empty vector (lanes 1, 4, and 7), 5 μg pEF-BOS-ΔRI-HA^2-hHus1, 5 μg pcDNA3-hRad1-FLAG^2, and 30 μg pcDNA3-AU1^2-hRad9 expression vector together (lanes 2, 5, 8), or with 5 μg pcDNA3-hRad1-FLAG^2 and 30 μg pcDNA3-AU1^2-hRad9 only (lanes 3, 6, 9). A portion of the lysate was prepared for SDS-PAGE, and the remainder was immunoprecipitated with anti-FLAG or anti-GFP. The cell lysates and immunoprecipitates were resolved by SDS-PAGE (10% gel), transferred to Immobilon P, and immunoblotted sequentially with **(C)** anti-FLAG and **(B)** anti-HA mAbs, followed by immunoblotting with **(A)** anti-GFP antiserum.

3.7   hRad9 is phosphorylated in response to DNA damage

DNA damage is not a requirement for interaction of the checkpoint proteins hRad9, hHus1, and hRad1. The *S. pombe* homolog of hHus1 (spHus1) is inducibly phosphorylated by treatment with DNA-damaging agents as a consequence of checkpoint pathway activation (Kostrub et al., 1998). scDdc1, the putative *S. cerevisiae* homolog of spRad9/hRad9 is also phosphorylated in response to DNA-damaging agents (Longhese et al., 1997). Because this phosphorylation requires the presence of other checkpoint gene products, a direct correlation between Ddc1 phosphorylation and activation of DNA damage checkpoints was proposed (Paciotti et al., 1998).

To assess, whether the human checkpoint protein hRad9 also participates in DNA damage-dependent phosphorylation cascades, we explored the possibility that hRad9 is also

phosphorylated in response to DNA damage. It is important to note that endogenous hRad9 (although highly modified) migrates as a single band when isolated from undamaged cells. We noticed that the single endogenous hRad9 band (70-kDa form) exhibited a progressively greater reduction in electrophoretic mobility when isolated from cells irradiated with increasing doses of IR (Fig. 8A). We also explored the time course of the DNA damage-induced mobility shift. It showed that hRad9 was modified within 30 min after treatment with IR, was maximal at 2 hrs, and persisted for at least 6 hrs (Fig. 8B). To determine whether the mobility shift reflected DNA damage-induced phosphorylation of the checkpoint protein, we treated hRad9 immunoprecipitates isolated from irradiated cells with calf intestinal phosphatase (Fig. 8C). As expected for phosphorylation, the DNA damage-induced mobility shift was readily reversed by treatment with the phosphatase. Moreover, inclusion of the phosphatase inhibitor beta-glycerophosphate blocked the effects of the phosphatase, suggesting that effects of the phosphatase preparation are not the result of contaminating activities. Under identical conditions we did not detect any shift in electrophoretic mobility of hHus1 and hRad1, suggesting that these proteins remain unphosphorylated in humans following treatment with IR (data not shown). Viewed together, these results strongly suggest that endogenous hRad9, in addition to other modifications, is modified by DNA damage-induced phosphorylation.
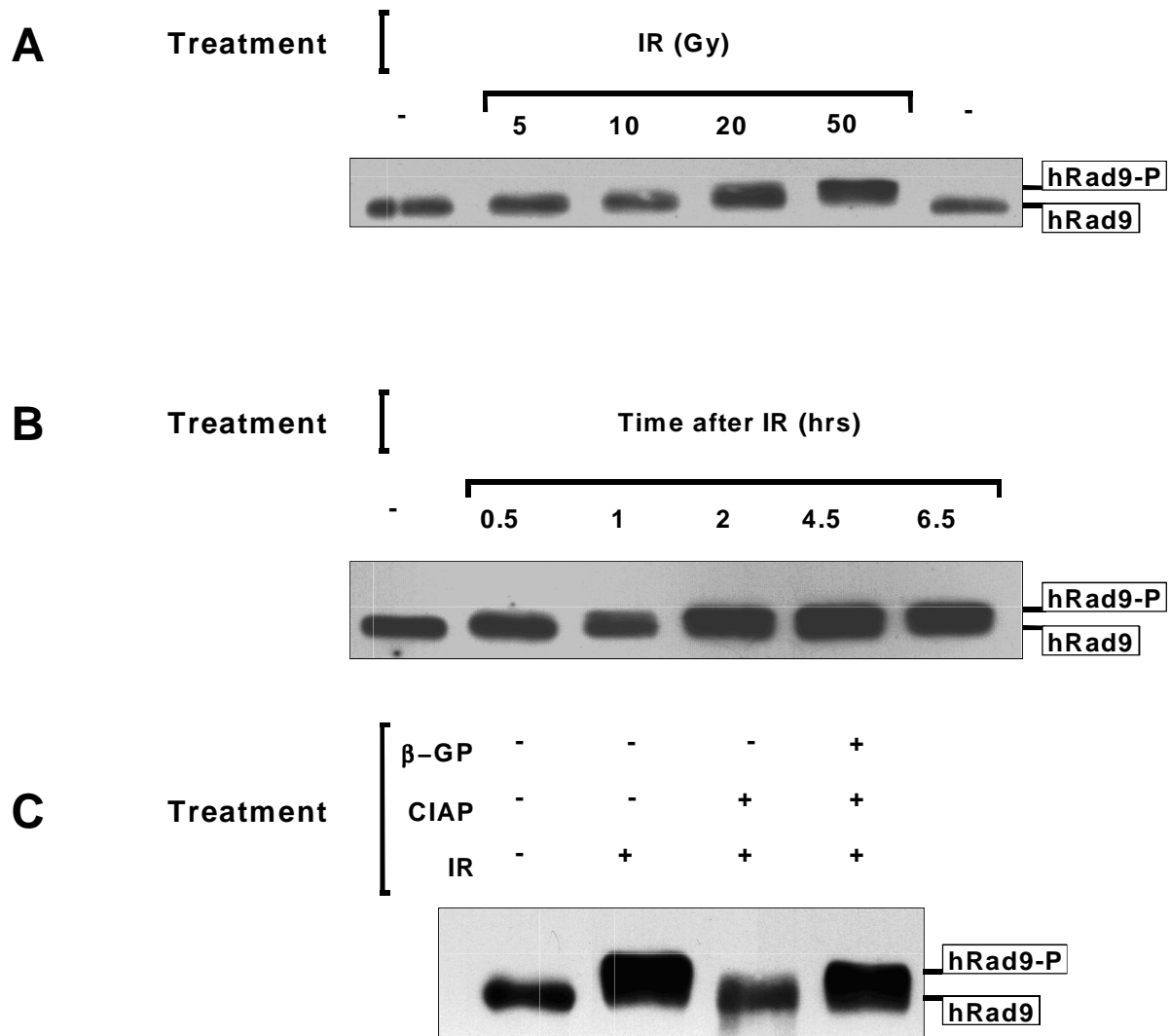
Figure 8. hRad9 is phosphorylated in response to DNA damage. **(A)** K562 cells (1×10^7 per sample) were treated with 5, 10, 20, or 50 gy IR or were left untreated (-) and cultured for 5 hrs after irradiation. Cell lysates were then immunoprecipitated with anti-hRad9, resolved by SDS-PAGE (10% gel), transferred to Immobilon P and blotted with anti-hRad9. **(B)** K562 cells (1×10^7 per sample) were either treated with 50 gy IR or were left untreated (-) and cultured for 0.5, 1, 2, 4.5, or 6.5 hrs. Cell lysates were then prepared and processed as in **(A)**. **(C)** Exponentially growing K562 cells (1×10^7 per sample) were treated with 0 (-) or 50 gy (+) IR, cultured for 5 hrs, and lysed. The lysates were immunoprecipitated with anti-hRad9. The immunoprecipitates were then washed with lysis buffer, followed by phosphatase buffer, and treated with 0.25 units calf intestinal alkaline phosphatase or were left untreated, in the absence and presence of 50 mM β-glycerophosphate, as indicated, for 30 min at 30°C. After phosphatase treatment the immunoprecipitates were washed once with lysis buffer, mixed with SDS-PAGE sample buffer, and resolved by SDS-PAGE (10% gel).

3.8 Phosphorylated hRad9 interacts with hHus1 and hRad1

Phosphorylation of the *S. pombe* checkpoint protein spHus1 in response to treatment with DNA-damaging agents does not alter spHus1's ability to bind to spRad1 (Kostrub et al., 1998). Likewise, phosphorylation of the *S. cerevisiae* hRad9 homolog (scDdc1) does not affect its interaction with the checkpoint protein scMec3 (Paciotti et al., 1998). We thus investigated whether IR-inducible hRad9 phosphorylation affects its binding to the hHus1-hRad1 complex. Figure 9 shows non-phosphorylated hRad9 from untreated cells (Fig. 9, lane 1) in comparison to phosphorylated hRad9 from cells treated with IR (Fig. 9, lane 2). Immunoprecipitation of hHus1 and hRad1 from non-irradiated cells and subsequent blotting with anti-hRad9 antiserum revealed association with hRad9 (Fig. 9, lanes 3 and 4) as observed in Figure 1. Immunoprecipitation of hRad1 and hHus1 from cells that were irradiated similarly yielded associated hRad9 protein (Fig. 9, lanes 5 and 6). All of the hRad9 detected appeared to be shifted, suggesting that the majority of the cellular hRad9 pool becomes phosphorylated in response to IR. These data further suggest that DNA damage does not alter the stoichiometry of the hRad9, hHus1, and hRad1 interaction.
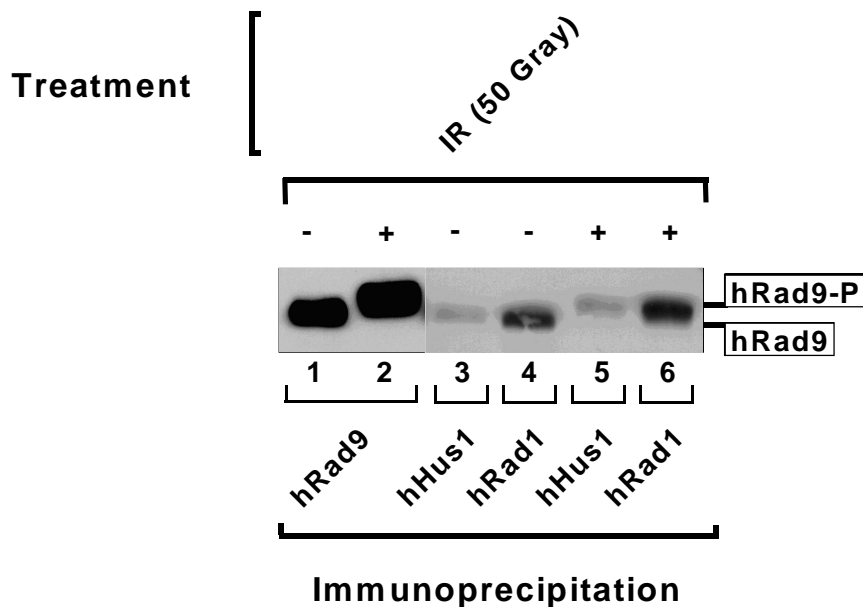

Figure 9. Phosphorylated hRad9 interacts with hHus1 and hRad1. K562 cells (1×10^7 per sample) were treated with 0 (-) or 50 gy (+) IR and cultured for 5 hrs after irradiation. Cell lysates were then immunoprecipitated with anti-hRad9 (lanes 1 and 2), with anti-hHus1 (lanes 3 and 5), or with anti-hRad1 (lanes 4 and 6), resolved by SDS-PAGE (10% gel), transferred to Immobilon P and blotted with anti-hRad9.

3.9 UV light induces moderate phosphorylation of hRad9 in K562 cells

Many checkpoint genes were identified by genetic analysis of radiosensitive yeast mutants (Elledge, 1996; Paulovich et al., 1997). *S. pombe* with mutant *sprad9* are sensitive to IR as well as to ultraviolet (UV) light, suggesting that spRad9 carries out functions in IR- and UV light-induced DNA damage responses. Expression of hRad9 in spRad9 mutant yeast did not complement UV light sensitivity or the UV-inducible G2-M checkpoint. In contrast, human Rad9 partially restored the survival of a G2-M checkpoint-defective *S. pombe* strain lacking spRad9 (Lieberman et al., 1996). This suggests that the human Rad9 protein may have lost its function in UV-induced damage response in humans. To test whether UV light induces phosphorylation of hRad9, and thus activates hRad9-dependent damage responses, we irradiated K562 cells with increasing doses of UV light and analyzed hRad9's ability to undergo phosphorylation. Whereas IR induced phosphorylation of most of the cellular hRad9 pool (Fig. 10, lane 2), UV irradiation generates only moderate phosphorylation of the hRad9 protein (Fig. 10, lanes 3-5), suggesting that additional mechanisms regulate the response to DNA damage induced by UV light in human cells.
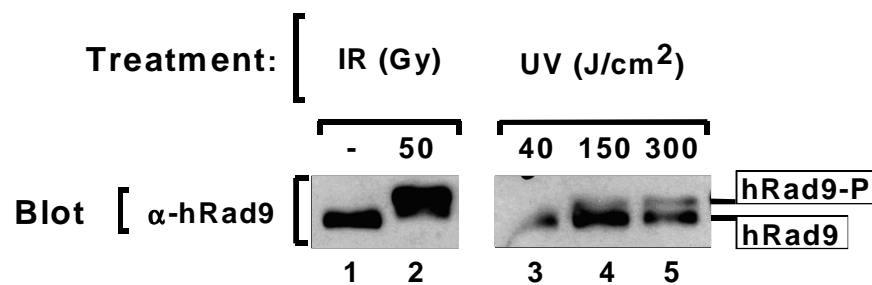

Figure 10. UV light induces only marginal phosphorylation of hRad9 in K562 cells. K562 cells (1×10^7 per sample) were treated with 0 (-) or 50 gy IR, or with 40, 150, and 300 J/cm^2 and cultured for 5 hrs after irradiation. Cell lysates were then immunoprecipitated with anti-hRad9, resolved by SDS-PAGE (10% gel), transferred to Immobilon P and blotted with anti-hRad9.

3.10 γ-irradiation induces phosphorylation of hRad9 in human keratinocytes

The human skin is the main target organ of UV radiation. Keratinocytes must therefore have potent protective mechanisms preventing radiation-induced DNA damage. This notion raised the question whether phosphorylation of hRad9 occurs in human keratinocytes as observed in K562 cells.

To address this we irradiated human keratinocytes and K562 cells with IR and UV light and explored hRad9's ability to undergo phosphorylation (Fig. 11). hRad9 extracted from γ-irradiated keratinocytes had reduced mobility relative to non-irradiated cells (Fig. 11A, lane 1 vs. lane 2), which demonstrates that IR induces hRad9 phosphorylation in keratinocytes. In contrast, escalating doses of UV light did not shift hRad9's mobility in human keratinocytes (Fig. 11A, lanes 3-5), suggesting that this modification of hRad9 is not actively involved in UV-induced DNA damage response in this cell type.

To further analyze the phosphorylation of hRad9 observed after γ-irradiation in human keratinocytes, keratinocytes were exposed to increasing doses of IR and migration characteristics of hRad9 were examined (Fig. 11C). Unlike with K562 cells, higher doses of IR are required to fully shift hRad9 in keratinocytes (Fig. 7A). The time-course experiment demonstrates that hRad9 phosphorylation peaks as early as 1 hr after irradiation and decreases within the following 2 to 3 hrs (Fig. 11B). Thus, in keratinocytes hRad9 is more rapidly phosphorylated than in K562 cells, and this response is shorter lived than in K562 cells (Fig. 8B). These data suggest that the hRad9 phosphorylation in response to IR is a physiological reaction in human keratinocytes and probably other human tissue types as well. Because hRad9 phosphorylation cannot be induced by UV light in human keratinocytes, other pathways are proposed to respond to UV-induced DNA damage, especially in keratinocytes.
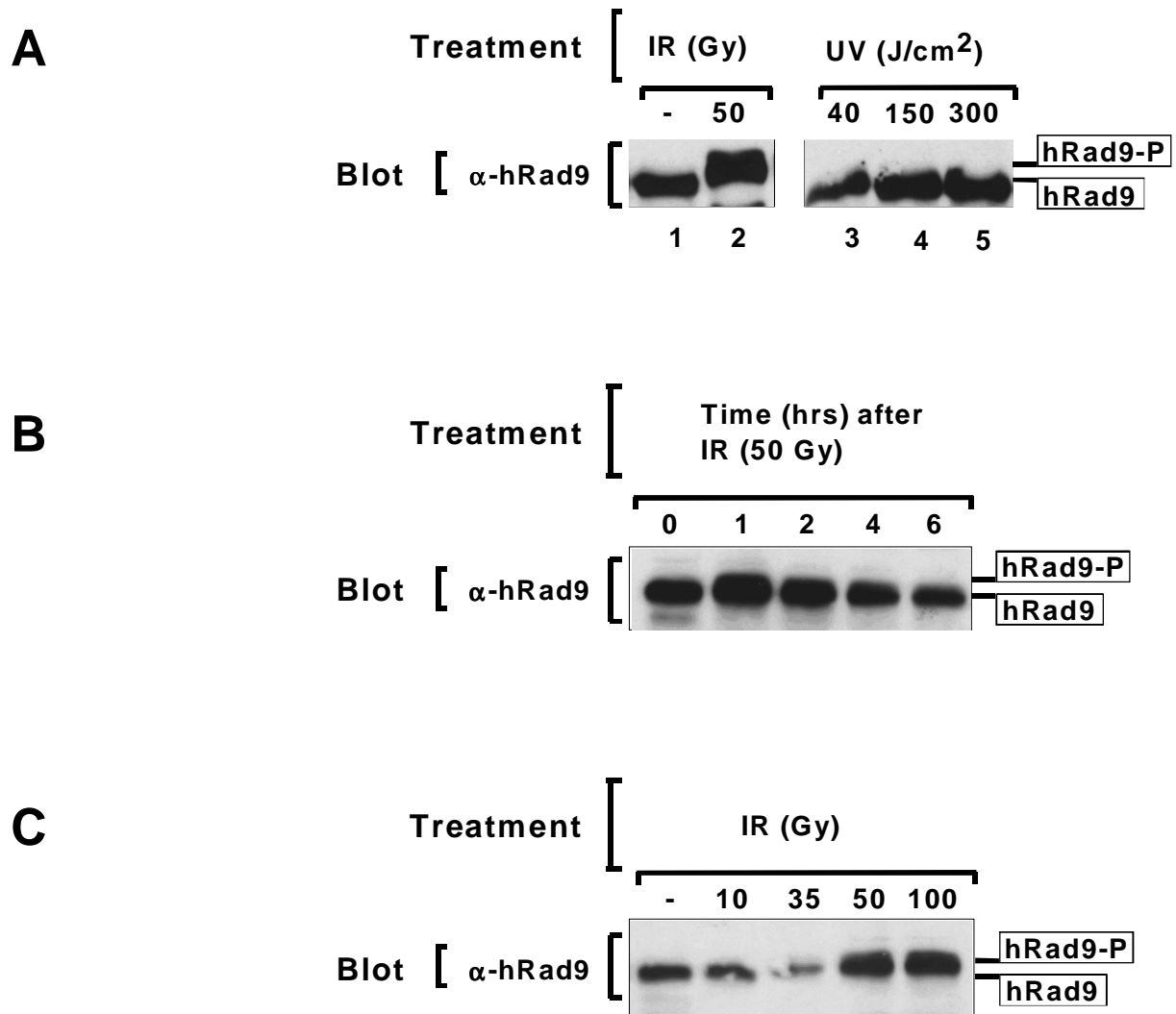
Figure 11. γ-irradiation - but not UV light - induces phosphorylation of hRad9 in human keratinocytes. **(A)** Human keratinocytes (5×10^6 per sample) were treated with 0 (-) or 50 gy IR, or with 40, 150, and 300 J/cm^2 UV light and cultured for 5 hrs after irradiation. Cell lysates were then immunoprecipitated with anti-hRad9, resolved by SDS-PAGE (10% gel), transferred to Immobilon P and blotted with anti-hRad9. **(B)** Human keratinocytes (5×10^6 per sample) were treated with 50 gray IR and cultured for 0, 1, 2, 4, or 6 hrs. Cell lysates were then immunoprecipitated with anti-hRad9, resolved by SDS-PAGE (10% gel), transferred to Immobilon P and blotted with anti-hRad9. **(C)** Human keratinocytes (5×10^6 per sample) were treated with 0 (-), 5, 10, 20, or 50 gy IR and cultured for 5 hrs after irradiation. Cell lysates were then immunoprecipitated with anti-hRad9, resolved by SDS-PAGE (10% gel), transferred to Immobilon P and blotted with anti-hRad9.

3.11 Epitope-tagged hRad9 is located in the nucleus

The previous data in combination with earlier studies in the yeasts *S. pombe* and *S. cerevisiae* support the idea that biochemical functions of hRad9 are conserved from lower eucaryotes to humans (Lieberman et al., 1996). The hRad9 homologs spRad9 (in *S. pombe*) and scDdc1 (in *S. cerevisiae*) are both components of checkpoint pathways activated by DNA damage (Longhese et al., 1997). Genetic and biochemical studies indicate that both spRad9 and scDdc1 function in close proximity to or directly in DNA damage detection, suggesting that these proteins may be located in the nucleus (Weinert, 1998; Longhese et al., 1998; Paciotti et al., 1998).

To assess where in the cell hRad9 is located, we transiently transfected K562 cells with either empty vector (Fig. 12A), green fluorescent protein (GFP) alone (Fig. 12B), or GFP-tagged hRad9 (Fig. 12C). The nuclei were counter-stained with the DNA-binding dye propidium iodide (PI), and cells were then analyzed using a confocal laser scanning microscope. In cells transfected with empty vector alone (Fig. 12A), the DNA-binding PI stain marked the nucleus (red). In cells transfected with GFP alone (Fig. 12B), GFP (green) was localized throughout the nucleus and the cytoplasm without any distinctive pattern. In contrast, cells transfected with hRad9-GFP (Fig. 12C) displayed a characteristic distribution of GFP-tagged hRad9, which was localized predominantly inside of the nucleus. Furthermore, we observed that GFP-tagged hRad9 was excluded from the nucleoli. Together, these results suggest that hRad9 is a nuclear protein, consistent with a proximal role in the detection of DNA damage or the relay of DNA damage-induced signals.
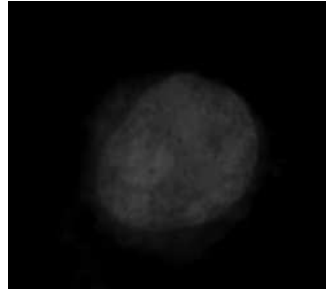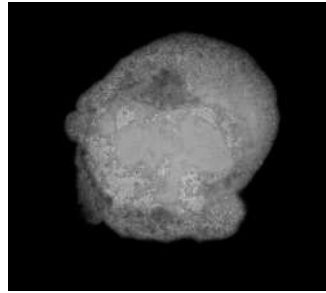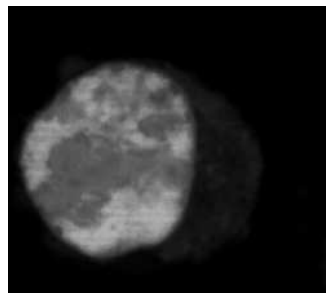
A   PI

B   PI and GFP

C   PI and GFP-tagged hRad9

Figure 12. Epitope-tagged hRad9 is located in the nucleus. K562 cells (5×10^6 per sample) were transfected with **(A)** empty vector, **(B)** 5 µg GFP alone, or **(C)** 5 µg GFP-tagged hRad9. Approximately 15000 cells of each sample were spun down on a microscopical coverslip and fixed with 4% paraformaldehyde in PBS for 3 min. Nuclei were counter-stained for 3 min with 10 µl/ml propidium iodide (PI) in PBS. Coverslips were air-dried and mounted on microscopic slides with Vectashield Antifade mounting medium. Fluorescent microscopy was performed using the Confocal laser scanning microscope LSM510. Images were created with the LSM510 software for windows NT and saved as TIFF files.

4 Discussion

The discovery of radiosensitive yeast mutants led to the cloning of the mutated genes (Rowley et al., 1992; al-Khodairy and Carr, 1992; Enoch et al., 1992). Some of these genes are clearly involved in DNA repair (Game, 2000). Others, dubbed checkpoint genes, participate in regulation of cell cycle control after DNA damage (Elledge, 1996; Paulovich et al., 1997). Their identification brought about a new paradigm of DNA damage response mechanisms in eucaryotes termed cell cycle checkpoints (Hartwell and Weinert, 1989). Checkpoints are signaling cascades that halt the cell cycle in response to DNA damage, thereby providing time for repair and preventing accumulation of DNA alterations. Thus, the coordination of checkpoint activation and DNA repair promotes genomic integrity throughout the cell cycle (Weinert, 1998; Elledge, 1996).

The recent identification of human homologs of yeast checkpoint proteins fueled speculation that the pathways regulating checkpoints may be conserved from yeast to humans (Udell et al., 1998; Savitsky et al., 1995; Lieberman et al., 1996; Parker et al., 1998; Kostrub et al., 1998; Sanchez et al., 1997). Checkpoint defects may generate genomic instability, which is characteristic and even diagnostic of virtually all human cancers (Elledge, 1996; Weinert, 1998; Longhese, 1998). In fact, some heritable instability syndromes that share predisposition to cancer as a common feature have defects in checkpoint-regulating genes, suggesting that intact checkpoint controls are crucial to prevent genomic instability and cancer (Kastan et al., 1995; Tainsky et al., 1995; Hoekstra, 1997). Although human homologs of checkpoint-regulating genes were identified, the physical and functional roles of many of these proteins are largely unexplored, even in the well-studied yeast systems.

The impact of checkpoint defects on genomic instability and carcinogenesis as well as the possibility to therapeutically exploit checkpoint defects in common cancers raises interest in the molecular mechanisms underlying checkpoint function. To gain insight into the functions of human checkpoint proteins, we have undertaken a biochemical and cellular analysis of the novel checkpoint proteins hRad9, hHus1, and hRad1. We show that hRad9 is a nuclear protein, which undergoes complex post-translational modifications in undamaged cells and is inducibly phosphorylated in response to DNA damage, indicating that this protein participates

in a DNA damage-inducible signaling pathway in humans. We also demonstrate that fully modified hRad9 interacts with hHus1 and hRad1 in a stable multimolecular complex that is present in damaged and even in undamaged cells. Unlike IR, our studies reveal that UV light only modestly induces hRad9 phosphorylation in K562 cells. In human keratinocytes, hRad9 is not phosphorylated in response to UV irradiation. These results demonstrate that hRad9, hHus1, and hRad1 form a stable IR-responsive checkpoint complex that actively participates in human cellular responses to DNA damage in K562 cells as well as in human keratinocytes.

4.1   A multi-component human checkpoint complex

Epistasis studies identify genetic interactions and are frequently indicative of biochemical interactions as well. Such studies in *S. cerevisiae* have shown genetic and biochemical interactions among the members of the *scrad24* epistasis group, which includes *S. cerevisiae* homologs for *hRAD1* (*scrad17*), *hRAD17* (*scrad24*), and *hRAD9* (*scddc1*; Longhese et al., 1997; Lydall and Weinert, 1995; Eckardt-Schupp et al., 1987). In addition, previous work demonstrated that spRad1 and spHus1 interacted in the fission yeast *S. pombe* (Kostrub et al., 1998). Although these studies demonstrated that spHus1 and spRad1 required spRad9 for interaction, which suggested that spRad9 might directly or indirectly tether the molecules, this possibility was not directly tested.

Using specific immunological reagents, our results demonstrate for the first time that the human proteins hRad9, hHus1, and hRad1 interact in a trimolecular complex. In contrast to previous studies in *S. pombe*, our studies suggest that hRad1 and hHus1 associate in the absence of hRad9. Several groups have since confirmed the interaction of these three proteins in cell lysates (St Onge et al., 1999; Caspari et al., 2000), in yeast two-hybrid systems (St Onge et al., 1999; Hang and Lieberman, 2000), in insect cells (Burtelow et al., 2001), and *in vitro* (Lindsey-Boltz et al., 2001; Griffith et al., 2002).

Because in our studies overexpressed, epitope-tagged hRad1 and hRad9 did not associate in the absence of co-expressed hHus1, and likewise, hHus1 and hRad9 could not associate without hRad1, we speculated that hRad1 and hHus1 alone form a heterodimeric complex that interacts with hRad9. Lately, reconstitution of the complex in insect cells revealed that each of the three members of the complex interacts with any other complex

member in a pair-wise manner, even without co-expression of the third binding partner. Mapping of the interaction domains indicated that the amino terminus of hRad9 interacts with the carboxyl terminus of hRad1, the amino terminus of hRad1 interacts with the carboxyl terminus of hHus1, and the amino terminus of hHus1 interacts with the carboxyl terminus of hRad9, suggesting that the three proteins form a ring-like structure (Burtelow et al., 2001). Given that we used overexpressed, epitope-tagged protein for our interaction studies, it seems likely that our epitope tags or the antibodies may have disrupted the interactions between hRad1 and hRad9 as well as between hHus1 and hRad9. Together, our results demonstrate that hRad9, hHus1, and hRad1 form a trimolecular complex in human cells. Furthermore, they suggest that human checkpoint complexes may be differentially assembled as compared to complexes in yeast cells, indicating that specific details in checkpoint function have changed, whereas general functions are conserved from yeast to humans.

4.2   hRad9 is extensively modified

The present studies revealed that endogenous hRad9 migrates with an apparent molecular mass of 70 kDa, whereas its predicted molecular mass is 45 kDa. Because endogenous hRad9 migrates anomalously even when isolated from untreated cells, the modification likely occurs in the absence of DNA damage. Initial insight into the discrepancy came from studies showing that expression of epitope-tagged hRad9 alone yielded a protein that migrated primarily as a 55-kDa band. Although the 55-kDa band is significantly larger than the predicted molecular mass (even when the 2-kDa epitope tag is taken into account), we could not determine whether this band represented an unmodified or partially modified form of hRad9.

Even more intriguing is the observation co-expression of hRad1 and hHus1 leads to the appearance of greater amounts of fully shifted protein. One possible explanation for this result is that hRad1 and hHus1 are required for hRad9 modification. Another, perhaps more plausible explanation is that hRad9 is not stable when overexpressed singly, but once it associates with hRad1 and hHus1 it forms a stable multimolecular complex. In support of this possibility, AU1-tagged hRad9 expresses less well than hRad9 fused to the large and stable GFP moiety.

It is more difficult to detect intermediate forms of modified AU1-hRad9 than of GFP-hRad9 (Karnitz, personal communication).

There is precedence for other checkpoint proteins undergoing extensive modifications that dramatically alter their apparent molecular mass and regulate their interactions with other proteins. For example, the unrelated scRad9 is phosphorylated in undamaged cells, and this modification is essential for scRad9's interaction with the checkpoint protein kinase scRad53 (Sun et al., 1998; Vialard et al., 1998). There are several potential molecular modifications that may contribute to hRad9's mobility shift, including phosphorylation. In fact, recent studies demonstrated that the anomalous migrating behavior of hRad9 is due to constitutive phosphorylation (Chen et al., 2001; St Onge et al., 2001). Apparently, high concentrations of phosphatase are necessary in order to achieve full reversal of this type of hRad9 phosphorylation, yielding a 45-kDa band representing unmodified hRad9. Our studies used low concentrations of phosphatase, which only reversed the inducible (hyper-) phosphorylation in response to IR. Thus, in addition to being inducibly phosphorylated in response to DNA damage, hRad9 is constitutively phosphorylated in the absence of genotoxic stress.

Several sites of constitutive phosphorylation have now been identified within the carboxyl terminus of the hRad9 protein (Roos-Mattjus et al., 2003; St Onge et al., 2003). By mutating the constitutively phosphorylated amino acids of hRad9 to alanins, it has been shown that constitutive hRad9 phosphorylation promotes cell survival when cells are exposed to genotoxic stress. Cells defective in constitutive hRad9 phosphorylation are unable to induce activation of Chk1 in response to genotoxins and are thus unable to induce Chk1-mediated checkpoint responses, indicating that hRad9's C-terminus is a regulatory region for effector functions of the hRad9-hHus1-hRad1 complex (Roos-Mattjus et al., 2003).

4.3 hRad9 is part of a DNA damage-responsive complex

Previous studies in yeast demonstrated that hRad1 and hHus1 genetically and biochemically interact and are required for activation of checkpoints in response to DNA damage and replication inhibitors (Kostrub et al., 1998). Although much genetic evidence attests to their importance in cell cycle arrest and survival, even in the well-studied yeast models little is known about their functions. spRad1 and hRad1 have significant homology

with *Ustilago maydis* Rec1, a putative exonuclease (Udell et al., 1998; Parker et al., 1998; Freire et al., 1998). Additionally, hRad1 and hRad9 may possess 3' to 5' exonuclease activity (Bessho and Sancar, 2000; Parker et al., 1998). The presence of DNA-metabolizing proteins in the multimolecular complex, coupled with genetic data that place spRad9, spHus1, and spRad1, and their *S. cerevisiae* counterparts early in the response pathway, suggests that the complex may function as a sensor that scans the genome for damaged DNA (Weinert, 1998; Longhese et al., 1998; Paciotti et al., 1998). Once damaged DNA is detected, this complex may initiate endonucleolytic processing of the lesions and trigger interactions with downstream signaling elements. Alternatively, the checkpoint complex may link unknown damage recognition components to downstream signal-transducing pathways that include ATM and hChk1, both of which are implicated in actively enforcing cell cycle arrest after DNA damage (Carr, 1996; Weinert, 1997).

The present results support an early role for hRad9 in evolutionarily conserved DNA damage-induced signaling cascades. In addition to being constitutively phosphorylated in the absence of DNA damage, a process required for activation of Chk1 (Roos-Mattjus et al., 2003), hRad9 is inducibly phosphorylated in response to IR (Volkmer and Karnitz, 1999; St Onge et al., 1999). Likewise, the yeast checkpoint protein scDdc1 (homolog of spRad9 and hRad9) is phosphorylated in response to IR (Longhese et al., 1997). scDdc1 phosphorylation requires MEC1, an ATM homolog (Paciotti et al., 1998), suggesting that scDdc1/hRad9 may be a key regulator of the complex. Interestingly, it was recently shown that IR-inducible hRad9 phosphorylation occurs on Ser272 and that this event is mediated by the checkpoint kinase ATM. Overexpression of hRad9-Ser272A mutant protein in human fibroblasts induces an increased sensitivity to IR and disturbs G1-S checkpoint induction, suggesting that hRad9 also participates in an IR-induced, ATM-mediated checkpoint activation (Chen et al., 2001).

Consistent with an early function in DNA damage response, the hRad9-hHus1-hRad1 complex has recently been shown to associate with chromatin after DNA damage (Burtelow et al., 2000). Furthermore, under refined experimental conditions, it could be demonstrated that the trimolecular complex interacts with hRad17, one of the six proteins that regulate checkpoint responses *S. pombe* (Rauen et al., 2000). Interestingly, hRad17 has extensive homology with all five subunits of replication factor C (RFC; Parker et al., 1998; Griffith et al.,

2002). RFC is a heteropentameric protein complex composed of one large (p140) and four smaller (p36, p37, p38, p40) subunits (Stillman, 1994). Competing with the largest subunit, hRad17 forms a complex with the four smaller RFC subunits (Lindsey-Boltz et al., 2001). It is well established that the original RFC complex loads proliferating cell nuclear antigen (PCNA), a trimolecular ring-like sliding clamp, onto DNA in a clamp-clamp loader-like fashion, which then tethers protein kinase C δ to DNA during DNA synthesis (Waga and Stillman, 1998). Based on biochemical data indicating that hRad9, hHus1, and hRad1 form a trimolecular complex *in vivo* (Volkmer and Karnitz, 1999; St Onge et al., 1999) with a putative ring-like structure (Burtelow et al., 2001), in combination with molecular modeling studies, which, based on sequence homology of each of the three complex members with PCNA, predicted that the hRad9-hHus1-hRad1 complex resembles PCNA, it has been suggested that hRad17-RFC may load the hRad9-hHus1-hRad1 ring onto DNA analogously to RFC and PCNA (Venclovas and Thelen, 2000; Caspari et al., 2000). Indeed, it could be demonstrated that the binding of the hRad9-hHus1-hRad1 complex to chromatin in response to DNA damage requires the presence of hRad17 (Zou et al., 2001) and, just recently, electron microscopic evidence was provided demonstrating that hRad17 recruits the hRad9-hHus1-hRad1 complex onto DNA in an ATP-dependent manner, suggesting that hRad17 may be the sensor of DNA damage, which then loads the checkpoint complex onto sites of damaged DNA (Bermudez et al., 2003). Taken together, the present data provide the first identification of a DNA damage-responsive human checkpoint complex that is fundamentally conserved between yeast and humans.

4.4 UV light is not a potent activator of hRad9 phosphorylation

Many checkpoint proteins were identified by genetic analysis of yeast mutants that were hypersensitive to genotoxic agents (Elledge, 1996; Paulovich et al., 1997). *S. pombe rad9* mutants are sensitive to IR, UV light, and hydroxyurea (HU). The human Rad9 protein, if expressed in an *S. pombe rad9* mutant strain, partially restores the IR-induced checkpoint responses and restores HU-induced checkpoint responses to nearly wild-type levels (Lieberman et al., 1996). These findings strongly suggest functional conservation of hRad9 from yeast to humans, at least in the HU- and IR-induced checkpoint response. Expression of hRad9 in spRad9 mutant yeast did not complement UV light-induced checkpoint delay at the

G2-M border (Lieberman et al., 1996). This may suggest that the Rad9 protein has lost its function in UV-induced damage response in humans. To test whether hRad9 participates in UV light-induced checkpoint response in humans, we irradiated K562 cells with increasing doses of UV light and analyzed whether UV induced hRad9 phosphorylation. Even at high doses, UV light only partially shifted hRad9's mobility. In marked contrast, UV light did not induce phosphorylation of hRad9 in keratinocytes, whereas IR did cause hRad9 phosphorylation in these cells.

These data suggest that hRad9 phosphorylation in response to IR is a physiological reaction in human keratinocytes and probably all other human tissue types as well. As UV light in human keratinocytes cannot trigger inducible phosphorylation other pathways are likely to respond to UV-induced DNA damage in these cells. We propose that keratinocytes, which are constantly exposed to UV light, may have evolved highly efficient mechanisms to immediately manage UV-induced DNA damage before checkpoint mechanisms are activated. In support of this hypothesis, inducible phosphorylation of hRad9 has been implicated in ATM-mediated checkpoint activation in response to IR, but not UV light, suggesting that hRad9 is not involved in UV-induced checkpoint responses (Chen et al., 2001). However, constitutive phosphorylation of hRad9 is required for activation of Chk1 in response to UV light, but not IR, indicating that different portions of hRad9 are involved in different checkpoints, which are activated by different types of DNA damage (Roos-Mattjus et al., 2003).

4.5   Checkpoint genes are potential candidates for tumor suppressor genes

While dominant-acting oncogenes can be activated by single mutations in one allele, tumor suppressor genes are usually recessive and require inactivating mutations in both alleles to develop their carcinogenic potential (Aaronson, 1991). Tumor suppressors may also cause hereditary cancer predisposition. An individual that is carrier of a defective allele in a tumor suppressor is phenotypically normal but has an increased risk to develop cancer because only one mutation in the remaining allele is necessary to inactivate the gene (Sherr, 1996). In these individuals, a single mutation in a tumor suppressor may be silent for years. This main

characteristic identifies tumor suppressors: genes that are required for normal cell function, and when defective initiate cancer development.

Interestingly, tumor suppressor gene products usually impose constraints on cell cycle progression or cell growth. Loss-of-function mutations release the constraints and subsequently promote genomic instability and carcinogenesis, which is consistent with a function in cell cycle checkpoints (Jacks and Weinberg, 1996). In fact, the classical tumor suppressor genes encode components of cell cycle checkpoints. Moreover, they are frequently mutated and lost in human cancers, suggesting that mutations of these stability genes during tumorigenesis may trigger cancer development (Donehower, 1997). To date, approximately ten tumor suppressor genes are known; the best characterized are *p53* and *RB*. Others, like the *ATM* or the *BRCA1* gene, are under investigation. Germ-line mutations within p53 or ATM cause the hereditary diseases Li-Fraumeni (LF) and ataxia telangiectasia (AT), which provoke genomic instability and were therefore termed instability syndromes (Kastan et al., 1995; Tainsky et al., 1995; Hoekstra, 1997). Germ-line mutations of the breast cancer susceptibility gene 1 (*BRCA1*) predispose women to breast and ovarian cancer. A role for this gene in DNA repair has been proposed recently, but *BRCA1* may also be involved in cell cycle checkpoint control (Feunteun and Lenoir, 1996; Xu et al., 1999; Paterson, 1998). It remains unclear, whether BRCA1's role in DNA repair or its role in cell cycle control or a combination of the two is responsible for the elevated risk of cancer. These studies indicate that disruption of DNA damage-activated cell cycle arrest may lead to increased cancer susceptibility as known for defects in DNA repair mechanisms.

The results of this study support the assumption that hRad9, hHus1, and hRad1 are important players in a signaling cascade that leads to cell cycle arrest. Given that hRad9, hHus1, and hRad1 have central roles in checkpoint activation, the absence of functional gene products would interrupt the downstream pathway and may impede checkpoint activation and thereby induce genomic instability. As a consequence, the rate of acquisition of mutations could increase dramatically and cause cancer, similar to defects in ATM or p53. An appropriate way to find out whether they are tumor suppressor genes would be to screen tumor cell populations for expression mutations. In fact, mutated hRad17, another checkpoint protein, is overexpressed in human non-small cell lung cancer cells, suggesting a role for

hRAD17 in tumor development (Sasaki et al., 2001). Although no mutations have yet been found in *hRAD9, hHUS1, and hRAD1*, studies in fission yeast show that lack of spRad1, spRad9, or spHus1 abolishes the G2 checkpoint, which induces increased sensitivity to genotoxic agents (Carr, 1994; Paulovich et al., 1997). Interestingly, the 11q 13 region, in which hRad9 resides, exhibits loss of heterozygosity in human cancers. At least two tumor suppressor loci were mapped to that region. The most prominent gene is *MEN1*, which is responsible for type 1 endocrine neoplasia. Fine resolution mapping data suggested that *hRAD9* is not the origin of this cancer syndrome (Lieberman et al., 1996). The presence of a second tumor suppressor locus in that region is suggested by studies on cervical cancer cell lines, and *hRAD9* remains a possible candidate for this tumor suppressor gene (Lieberman et al., 1996). In like manner, *hRAD1* has been mapped to a region that is associated with a tumor suppressor locus in human lung and bladder cancer (Parker et al., 1998; Marathi et al., 1998). These data suggest that *hRAD9*, *hRAD1*, and possibly other human checkpoint genes may act as tumor suppressor genes analogous to *p53* and *ATM*. Further experiments, particularly the cloning of the homologous mouse cDNA and generation of knock out mice and tumor cell screens, will clarify this issue.

4.6 Therapeutic exploitation of checkpoint research: Perspectives for checkpoint-based cancer therapy

The identification of key participants in the DNA damage checkpoint pathway raises the possibility of the development of checkpoint-based chemotherapy. More than 50% of all human malignant tumors contain mutated p53, and p53-deficient (p53$^-$) tumor cells lack a DNA damage-induced G1-S checkpoint (Lutzker and Levine, 1996). Loss of p53 function also has variable effects on radiosensitivity and chemosensitivity. In some p53$^-$ tumor cell lines, genotoxic agents do not induce apoptosis resulting in decreased sensitivity to γ-irradiation or chemotherapeutics compared to normal cells (Kastan et al., 1995). In many other cases, loss of p53 has no effect on the sensitivity of a tumor cell to γ-irradiation (Lutzker and Levine, 1996). One emerging hypothesis is that pharmacological agents that disrupt the G2 checkpoints would preferentially radiosensitize p53$^-$ (G1-S checkpoint-lacking) tumor cells by disrupting potentially compensating G2 checkpoints (Powell et al., 1995). In fact, selective G2 checkpoint abrogators like methylxanthines (caffeine and pentoxifylline) selectively increased

killing of p53-deficient tumor cells by γ-irradiation (Russel et al., 1996). Unfortunately, efficient doses of caffeine are too toxic for human therapy, and tolerable plasma levels of pentoxifylline are well below doses that suffice for G2 checkpoint abrogation *in vitro*. Another selective G2 checkpoint abrogator, UCN-01 (7-hydroxystaurosporine), is currently undergoing clinical trials for cancer treatment (Sausville et al., 2001). It was shown that this drug increased killing of p53-deficient tumor cells by γ-irradiation (Wang et al., 1996). Interestingly, the G2 checkpoint abrogation is mediated by inhibition of Chk1, one of the conserved fission yeast checkpoint proteins, suggesting that other checkpoint proteins may be targets for drugs in cancer therapy as well (Busby et al., 2000; Graves et al., 2000).

To devise other rational ways to intervene with checkpoint-based chemotherapy, we need to understand the mechanism of checkpoint activation. This study provides an initial step towards the elucidation of checkpoint function in humans. Given that hRad9 is a key regulator of G2 checkpoints in humans as suggested by corresponding studies in yeast, and hRad9 phosphorylation is the initiating step to promote checkpoint activation, it may suffice to block the kinase that phosphorylates hRad9 to inhibit G2 checkpoint activation. Inhibition of hRad9 phosphorylation may thus serve to abrogate G2 checkpoint activation and enhance killing of p53-deficient tumor cells. A screen for substances blocking hRad9 activation could provide a broad spectrum of potential chemotherapeutics of use in checkpoint-based therapy. Although these projects will require extensive efforts in the future, the discoveries presented here support checkpoint research fundamentally to unravel the underlying mechanisms. This may help to facilitate the identification of new strategies in cancer therapy.

5 Summary

Human cells have evolved protective mechanisms such as DNA repair and cell cycle checkpoints in order to promote stability of the genome. Studies on hereditary instability syndromes associated with a higher incidence of malignancies like Xeroderma pigmentosum or Nijmegen breakage syndrome demonstrated that genetic defects and subsequent dysfunction of a specific DNA repair mechanism trigger the development of cancer. Within the last years, the investigation of cell cycle checkpoints gained increasing importance in cancer research.

Checkpoints are signaling cascades that halt the cell cycle in response to DNA damage, thereby providing time for repair and preventing accumulation of DNA alterations. While the p53-dependent G1-S checkpoint has been extensively investigated, little is known about other checkpoints in humans such as the G2-M or the S-phase progression checkpoint. Studies on the human cancer syndrome ataxia telangiectasia (AT) showed that AT cells fail to induce several checkpoints in response to ionizing radiation (IR), indicating that a checkpoint gene defect is responsible for the AT-associated cancers. The responsible gene (*ATM*) has significant sequence homology to the checkpoint kinase gene *sprad3* in the fission yeast *Schizosaccharomyces pombe* (*S. pombe*). In *S. pombe*, spRad3 regulates G2-M checkpoint activation in response to DNA damage. Defects in the *sprad3* gene, like defects in *ATM*, sensitize the organisms to radiation and radiomimetic drugs, suggesting conservation of checkpoint pathways from yeast to humans as well as a potential role of the G2-M checkpoint in carcinogenesis.

The discovery of G2-M checkpoint-deficient yeast mutants led to the cloning of additional checkpoint genes in yeast and their human homologs. This group of novel human genes includes homologs of *sprad9* (*hRAD9*), *sphus1* (*hHUS1*), and *sprad1* (*hRAD1*). In *S. pombe*, these genes are required for activation of spRad3, and defects in one or more of these genes render the yeast more sensitive to genotoxic agents. Mutations within the human rad genes may bring about an increased rate of mutations and genomic instability as shown for p53 or AT and may be responsible for inherited predisposition to cancer.

In view of this potential importance of human rad genes in the process of carcinogenesis, we have undertaken a cellular and molecular analysis of the novel human checkpoint proteins hRad9, hHus1, and hRad1 in the leukemia cell line K562 and in human keratinocytes. Using specific antibodies to the hRad9, hHus1, and hRad1 proteins we demonstrated with co-immunoprecipitation and Western-blot experiments that the human checkpoint proteins hRad9, hHus1, and hRad1 associate in a biochemical complex similar to the spRad9-spHus1-spRad1 complex reported in fission yeast.

To generate a model system of checkpoint protein function amenable to biochemical analysis, we prepared epitope-tagged expression vectors for hRad9, hHus1, and hRad1, which were transfected into K562 cells by electroporation, resulting in transient expression of epitope-tagged protein. By simultaneous expression of hRad9, hHus1, and hRad1 we showed that transiently expressed epitope-tagged checkpoint proteins hRad9, hHus1, and hRad1 recapitulate complex formation of endogenous proteins. Immunoprecipitation studies with lysates of hRad9-overexpressing cells revealed that hRad9 undergoes complex post-translational modifications. Co-expression of hRad9 with hHus1, and hRad1 resulted in a large increase of the amount of a highly modified form of hRad9, suggesting that hRad1 and hHus1 either promote formation of, or stabilize the modified form of hRad9.

Previously, a direct correlation between checkpoint protein phosphorylation and activation of DNA damage checkpoints in yeast was proposed. In this study, we show that hRad9 is phosphorylated in response to DNA damage, and that phosphorylated hRad9 interacts with hHus1 and hRad1 as well. The present results suggest that the hRad9-hHus1-hRad1 complex actively participates in an evolutionarily conserved DNA damage-induced signaling cascade.

hRad1 seems to possess exonuclease activity. The presence of a putative DNA-metabolizing protein in the multimolecular checkpoint complex, coupled with genetic data that place spRad9, spHus1, and spRad1 early in the response pathway of checkpoint activation suggests that the complex may function as a sensor that scans the genome for damaged DNA. Once damaged DNA is detected, this complex may initiate endonucleolytic processing of the lesions and trigger interactions with downstream signaling elements, or may link unknown

damage recognition components to downstream signal-transducing pathways that include the ATM kinase, which is implicated in actively enforcing cell cycle arrest after DNA damage.

Potential goals of checkpoint research include the implementation of screening tests to identify familial cancer predisposition and treatment of checkpoint gene defects by gene transfer. Another aim of checkpoint research is the development of checkpoint-based cancer therapy. More than 50% of all human malignant tumors contain mutated p53, and p53-deficient tumor cells lack induction of the G1-S checkpoint in response to DNA damage. One emerging hypothesis is that selective inhibitors of the compensating G2-M checkpoint would preferentially radiosensitize p53-deficient tumor cells. Thus, the investigation of checkpoint function in humans provides further targets for chemotherapeutic agents and will help to design future strategies in cancer therapy.

6 Zusammenfassung

Um DNA-Mutationen und in der Folge die Krebsentstehung beim Menschen zu verhindern, besitzen Zellen Schutzmechanismen wie DNA-Reparatur und Zellzyklus-Checkpoints. Die Untersuchung hereditärer Instabilitätssyndrome wie Xeroderma pigmentosum oder Nijmegen Breakage Syndrome hat ergeben, dass Defekte in DNA-Reparaturgenen die Karzinogenese beschleunigen und eine erbliche Krebsprädisposition bedingen können. Neben den DNA-Reparaturmechanismen gewinnen Checkpoints in der Erforschung der Krebsentstehung und in der Krebstherapie zunehmend an Bedeutung.

Checkpoints sind Signalkaskaden, die als Folge eines DNA-Schadens aktiviert werden und den Zellzyklus an definierten Positionen verlangsamen oder stoppen. Dadurch wird Zeit für die Koordination der DNA-Reparatur gewonnen und so die Integrität des Genoms gewahrt. Während die Bedeutung des p53-abhängigen G1-S-Checkpoints mittlerweile unumstritten ist, weiß man bis heute wenig über andere Checkpoints beim Menschen wie zum Beispiel den G2-M- oder den S-Phase-Progressions-Checkpoint. Die Untersuchung des Instabilitätssyndroms Ataxia teleangiectatica (AT) hat gezeigt, dass γ-bestrahlte AT-Zellen nicht in der Lage sind, verschiedene Checkpoints zu induzieren. Diese Beobachtung ließ die Vermutung aufkommen, dass ein Checkpoint-Gendefekt für die Zunahme der Malignom-Inzidenz bei AT-Patienten ursächlich ist. Das verantwortliche Gen (*ATM*) ist ein Homolog des Checkpoint-Kinase-Gens *sprad3* der Spalthefe *Schizosaccharomyces pombe* (*S. pombe*). In *S. pombe* reguliert spRad3 die G2-M-Checkpoint-Aktivierung als zelluläre Antwort auf geschädigte DNA. Defekte im *sprad3*-Gen, ebenso wie Defekte im *ATM*-Gen, führen zu einer gesteigerten Empfindlichkeit des Organismus gegenüber Karzinogenen, was eine evolutionäre Konservierung der Checkpoint-Signalkaskaden von der Hefe zum Menschen sowie eine mögliche Rolle des G2-M-Checkpoints in der Krebsentstehung nahe legt.

Die Entdeckung G2-M-Checkpoint-defizienter Hefemutanten ermöglichte die Klonierung weiterer Hefe-Checkpoint-Gene und die Identifikation ihrer humanen Homologe. Diese neue Gruppe menschlicher Gene beinhaltet Homologe von *sprad9* (*hRAD9*), *sphus1* (*hHUS1*) und *sprad1* (*hRAD1*). In der Spalthefe *S. pombe* sind die Genprodukte von *sprad9*, *sphus1* und *sprad1* für die Aktivierung der Kinase spRad3 notwendig, und Defekte in einem

oder mehreren dieser Gene verursachen eine erhöhte Sensibilität gegenüber Mutagenen. Gendefekte in den humanen Homologen der rad-Gene könnten, wie im Falle von p53 oder Ataxia teleangiectatica, einen Anstieg der Mutationsrate bedingen und für eine erbliche Krebsprädisposition verantwortlich sein.

In Anbetracht dieser potenziellen Bedeutung menschlicher rad-Gene im Prozess der Karzinogenese wurde hier eine zelluläre und molekulare Analyse der neuen humanen Checkpoint-Proteine hRad9, hHus1 und hRad1 in der Leukämie-Zelllinie K562 und in menschlichen Keratinozyten unternommen. Mit Hilfe spezifischer Antikörper gegen humanes Rad9, Hus1 und Rad1 konnte in Ko-Immunopräzipitations- und Western-Blot-Experimenten demonstriert werden, dass sich hRad9, hHus1 und hRad1 zu einem biochemischen Komplex ähnlich dem in Spalthefe bekannten spRad9-spHus1-spRad1-Komplex verbinden.

Um ein Modellsystem zu schaffen, in dem die Funktionen der Checkpoint-Proteine analysiert werden können, wurden Epitop-markierte Expressionsvektoren für hRad9, hHus1 und hRad1 generiert. Diese wurden durch Elektroporation in K562-Zellen transfiziert, was zur transienten Expression der Epitop-markierten Proteine führte. Durch simultane Expression von hRad9, hHus1 und hRad1 konnte der Nachweis erbracht werden, dass die Epitop-markierten Checkpoint-Proteine hRad9, hHus1 und hRad1 die Komplexbildung der endogenen Proteine rekapitulieren. Anhand von Immunopräzipitations-Experimenten mit Lysaten hRad9 überexprimierender Zellen wurde belegt, dass hRad9 komplexen post-translationellen Modifikationen unterzogen wird. Die Ko-Expression von hRad9 mit hRad1 und hHus1 resultierte in einem Anstieg der Menge von hRad9 in seiner modifizierten Form, was suggeriert, dass hRad1 und hHus1 entweder die Produktion von stark modifiziertem hRad9 fördern oder aber die modifizierte Form von hRad9 stabilisieren.

Für die Hefe-Checkpoints konnte ein direkter Zusammenhang zwischen der Phosphorylierung von Checkpoint-Proteinen und der Aktivierung der Checkpoint-Signalkaskaden bewiesen werden. In dieser Studie konnte aufgedeckt werden, dass hRad9 in γ-bestrahlten Zellen phosphoryliert wird und dass phosphoryliertes hRad9 ebenso mit hRad1 und hHus1 interagiert. Dies weist darauf hin, dass der hRad9-hHus1-hRad1-Komplex ein aktives Element einer Checkpoint-Signalkaskade ist, die durch DNA-Schäden aktiviert wird.

Einige Studien lieferten Hinweise dafür, dass hRad1 Exonuklease-Aktivität besitzt. Die Tatsache, dass ein potenziell DNA-metabolisierendes Protein Bestandteil eines Checkpoint-Proteinkomplexes ist, in Verbindung mit den Ergebnissen genetischer Untersuchungen der Spalthefe *S. pombe*, die spRad9, spHus1 und spRad1 früh in den Prozess der zellulären Antwort auf geschädigte DNA einordnen, deutet darauf hin, dass der Komplex als Sensor für DNA-Schäden dienen könnte. Nach der Entdeckung geschädigter DNA könnte der Proteinkomplex die endonukleolytische Prozessierung der DNA-Läsionen initiieren und Interaktionen mit stromabwärts in der Signalkaskade fungierenden Elementen vermitteln. Alternativ könnte der Komplex bisher unbekannte Sensoren für geschädigte DNA an die Funktion der stromabwärts agierenden ATM-Kinase koppeln, welche aktiv den Zellzyklus anhält, sobald DNA geschädigt wird.

Mögliche Ziele der Checkpoint-Forschung sind beispielsweise die Behandlung von Checkpoint-Genmutationen mittels Gentransfer, der Einsatz von Screening-Tests zur Identifikation familiär prädisponierter Personengruppen oder die Entwicklung Checkpoint-basierter Krebstherapien. Dabei macht man sich zu Nutze, dass mehr als 50 % aller malignen Tumore auf Grund einer p53-Mutation nicht in der Lage sind, auf DNA-Schäden mit der Induktion des G1-S-Checkpoints zu reagieren. Selektive Inhibitoren des den G1-S-Checkpoint kompensierenden G2-M-Checkpoints bewirken eine gegenüber gesundem Gewebe gesteigerte Strahlen- und Chemosensibilität der Tumorzellen. So eröffnet die Checkpoint-Forschung durch die Entdeckung zusätzlicher molekularer Angriffspunkte für Chemotherapeutika neue Möglichkeiten in der Konzeption künftiger Krebstherapien.

7 References

1.   Aaronson SA (1991) Growth factors and cancer. Science 254: 1146-53

2.   al-Khodairy F, Carr AM (1992) DNA repair mutants defining G2 checkpoint pathways in Schizosaccharomyces pombe. Embo J 11: 1343-50

3.   al-Khodairy F, Fotou E, Sheldrick KS, Griffiths DJ, Lehmann AR, Carr AM (1994) Identification and characterization of new elements involved in checkpoint and feedback controls in fission yeast. Mol Biol Cell 5: 147-60

4.   Athma P, Rappaport R, Swift M (1996) Molecular genotyping shows that ataxia-telangiectasia heterozygotes are predisposed to breast cancer. Cancer Genet Cytogenet 92: 130-4

5.   Bao S, Shen X, Shen K, Liu Y, Wang XF (1998) The mammalian Rad24 homologous to yeast Saccharomyces cerevisiae Rad24 and Schizosaccharomyces pombe Rad17 is involved in DNA damage checkpoint. Cell Growth Differ 9: 961-7

6.   Bermudez VP, Lindsey-Boltz LA, Cesare AJ, Maniwa Y, Griffith JD, Hurwitz J, Sancar A (2003) Loading of the human 9-1-1 checkpoint complex onto DNA by the checkpoint clamp loader hRad17-replication factor C complex in vitro. Proc Natl Acad Sci U S A 100: 1633-8

7.   Bessho T, Sancar A (2000) Human DNA damage checkpoint protein hRAD9 is a 3' to 5' exonuclease. J Biol Chem 275: 7451-4

8.   Bishop J (1991) Molecular themes in oncogenesis. Cell 64: 235-248

9.   Burtelow MA, Kaufmann SH, Karnitz LM (2000) Retention of the human Rad9 checkpoint complex in extraction-resistant nuclear complexes after DNA damage. J Biol Chem 275: 26343-8

10. Burtelow MA, Roos-Mattjus PM, Rauen M, Babendure JR, Karnitz LM (2001) Reconstitution and molecular analysis of the hRad9-hHus1-hRad1 (9-1-1) DNA damage responsive checkpoint complex. J Biol Chem 276: 25903-9

11. Busby EC, Leistritz DF, Abraham RT, Karnitz LM, Sarkaria JN (2000) The radiosensitizing agent 7-hydroxystaurosporine (UCN-01) inhibits the DNA damage checkpoint kinase hChk1. Cancer Res 60: 2108-12

12. Canman CE, Lim DS, Cimprich KA, Taya Y, Tamai K, Sakaguchi K, Appella E, Kastan MB, Siliciano JD (1998) Activation of the ATM kinase by ionizing radiation and phosphorylation of p53. Science 281: 1677-9

13. Carr AM (1996) Checkpoints take the next step. Science 271: 314-5

14. Carr AM (1997) Control of cell cycle arrest by the Mec1sc/Rad3sp DNA structure checkpoint pathway. Curr Opin Genet Dev 7: 93-8

15. Caspari T, Dahlen M, Kanter-Smoler G, Lindsay HD, Hofmann K, Papadimitriou K, Sunnerhagen P, Carr AM (2000) Characterization of Schizosaccharomyces pombe Hus1: a PCNA-related protein that associates with Rad1 and Rad9. Mol Cell Biol 20: 1254-62

16. Chalfie M, Tu Y, Euskirchen G, Ward WW, Prasher DC (1994) Green fluorescent protein as a marker for gene expression. Science 263: 802-5

17. Chen MJ, Lin YT, Lieberman HB, Chen G, Lee EY (2001) ATM-dependent phosphorylation of human Rad9 is required for ionizing radiation-induced checkpoint activation. J Biol Chem 276: 16580-6

18. Christians FC, Newcomb TG, Loeb LA (1995) Potential sources of multiple mutations in human cancers. Prev Med 24: 329-32

19. Collins K, Jacks T, Pavletich NP (1997) The cell cycle and cancer. Proc Natl Acad Sci U S A 94: 2776-8

20. de Boer J, Hoeijmakers JH (2000) Nucleotide excision repair and human syndromes. Carcinogenesis 21: 453-60

21. Donehower LA (1997) Genetic instability in animal tumorigenesis models. Cancer Surv 29: 329-52

22. Eckardt-Schupp F, Siede W, Game JC (1987) The RAD24 (= Rs1) gene product of Saccharomyces cerevisiae participates in two different pathways of DNA repair. Genetics 115: 83-90

23. Elledge SJ (1996) Cell cycle checkpoints: preventing an identity crisis. Science 274: 1664-72

24. Enoch T, Carr AM, Nurse P (1992) Fission yeast genes involved in coupling mitosis to completion of DNA replication. Genes Dev 6: 2035-46

25. Fearon ER, Vogelstein B (1990) A genetic model for colorectal tumorigenesis. Cell 61: 759-67

26. Freire R, Murguia JR, Tarsounas M, Lowndes NF, Moens PB, Jackson SP (1998) Human and mouse homologs of Schizosaccharomyces pombe rad1(+) and Saccharomyces cerevisiae RAD17: linkage to checkpoint control and mammalian meiosis. Genes Dev 12: 2560-73

27. Furnari B, Rhind N, Russell P (1997) Cdc25 mitotic inducer targeted by chk1 DNA damage checkpoint kinase. Science 277: 1495-7

28. Game JC (2000) The Saccharomyces repair genes at the end of the century. Mutat Res 451: 277-93

29. Gatti RA (1991) Speculations on the ataxia-telangiectasia defect. Clin Immunol Immunopathol 61: S10-5

30. Graves PR, Yu L, Schwarz JK, Gales J, Sausville EA, O'Connor PM, Piwnica-Worms H (2000) The Chk1 protein kinase and the Cdc25C regulatory pathways are targets of the anticancer agent UCN-01. J Biol Chem 275: 5600-5

31. Griffith JD, Lindsey-Boltz LA, Sancar A (2002) Structures of the human Rad17-replication factor C and checkpoint Rad 9-1-1 complexes visualized by glycerol spray/low voltage microscopy. J Biol Chem 277: 15233-6

32. Guan KL, Dixon JE (1991) Eukaryotic proteins expressed in Escherichia coli: an improved thrombin cleavage and purification procedure of fusion proteins with glutathione S-transferase. Anal Biochem 192: 262-7

33. Hang H, Lieberman HB (2000) Physical interactions among human checkpoint control proteins HUS1p, RAD1p, and RAD9p, and implications for the regulation of cell cycle progression. Genomics 65: 24-33

34. Hartwell LH, Weinert TA (1989) Checkpoints: controls that ensure the order of cell cycle events. Science 246: 629-34

35. Hartwell L (1992) Defects in a cell cycle checkpoint may be responsible for the genomic instability of cancer cells. Cell 71: 543-6

36. Hartwell L, Weinert T, Kadyk L, Garvik B (1994) Cell cycle checkpoints, genomic integrity, and cancer. Cold Spring Harb Symp Quant Biol 59: 259-63

37. Hartwell LH, Kastan MB (1994) Cell cycle control and cancer. Science 266: 1821-8

38. Hartwell L (1995) 1994 forbeck cancer forum on cell cycle checkpoints. Clin Cancer Res 1: 1067

39. Hoeijmakers JH (2001) Genome maintenance mechanisms for preventing cancer. Nature 411: 366-74

40. Hoekstra MF (1997) Responses to DNA damage and regulation of cell cycle checkpoints by the ATM protein kinase family. Curr Opin Genet Dev 7: 170-5

41. Hsieh P (2001) Molecular mechanisms of DNA mismatch repair. Mutat Res 486: 71-87

42. Hunter T (1991) Cooperation between oncogenes. Cell 64: 249-70

43. Jacks T, Weinberg RA (1996) Cell-cycle control and its watchman. Nature 381: 643-4

44.   Jackson SP (2002) Sensing and repairing DNA double-strand breaks. Carcinogenesis 23: 687-96

45.   Kastan MB, Canman CE, Leonard CJ (1995) P53, cell cycle control and apoptosis: implications for cancer. Cancer Metastasis Rev 14: 3-15

46.   Kaufmann WK, Schwartz JL, Hurt JC, Byrd LL, Galloway DA, Levedakou E, Paules RS (1997) Inactivation of G2 checkpoint function and chromosomal destabilization are linked in human fibroblasts expressing human papillomavirus type 16 E6. Cell Growth Differ 8: 1105-14

47.   Kostrub CF, al-Khodairy F, Ghazizadeh H, Carr AM, Enoch T (1997) Molecular analysis of hus1+, a fission yeast gene required for S-M and DNA damage checkpoints. Mol Gen Genet 254: 389-99

48.   Kostrub CF, Knudsen K, Subramani S, Enoch T (1998) Hus1p, a conserved fission yeast checkpoint protein, interacts with Rad1p and is phosphorylated in response to DNA damage. Embo J 17: 2055-66

49.   Levine AJ (1997) p53, the cellular gatekeeper for growth and division. Cell 88: 323-31

50.   Lieberman HB, Hopkins KM, Nass M, Demetrick D, Davey S (1996) A human homolog of the Schizosaccharomyces pombe rad9+ checkpoint control gene. Proc Natl Acad Sci U S A 93: 13890-5

51.   Lindahl T, Wood RD (1999) Quality control by DNA repair. Science 286: 1897-905

52.   Lindsey-Boltz LA, Bermudez VP, Hurwitz J, Sancar A (2001) Purification and characterization of human DNA damage checkpoint Rad complexes. Proc Natl Acad Sci U S A 98: 11236-41

53.   Loeb LA (1991) Mutator phenotype may be required for multistage carcinogenesis. Cancer Res 51: 3075-9

54.   Loegering D, Arlander SJ, Hackbarth J, Vroman BT, Roos-Mattjus P, Hopkins KM, Lieberman HB, Karnitz LM, Kaufmann SH (2004) Rad9 protects cells from topoisomerase poison-induced cell death. J Biol Chem 279: 18641-7

55.   Longhese MP, Paciotti V, Fraschini R, Zaccarini R, Plevani P, Lucchini G (1997) The novel DNA damage checkpoint protein ddc1p is phosphorylated periodically during the cell cycle and in response to DNA damage in budding yeast. Embo J 16: 5216-26

56.   Longhese MP, Foiani M, Muzi-Falconi M, Lucchini G, Plevani P (1998) DNA damage checkpoint in budding yeast. Embo J 17: 5525-8

57.   Lozzio BB, Lozzio CB (1977) Properties of the K562 cell line derived from a patient with chronic myeloid leukemia. Int J Cancer 19: 136

58. Lutzker SG, Levine AJ (1996) Apoptosis and cancer chemotherapy. Cancer Treat Res 87: 345-56

59. Lydall D, Weinert T (1995) Yeast checkpoint genes in DNA damage processing: implications for repair and arrest. Science 270: 1488-91

60. Marathi UK, Dahlen M, Sunnerhagen P, Romero AV, Ramagli LS, Siciliano MJ, Li L, Legerski RJ (1998) RAD1, a human structural homolog of the Schizosaccharomyces pombe RAD1 cell cycle checkpoint gene. Genomics 54: 344-7

61. Marshall CJ (1991) Tumor suppressor genes. Cell 64: 313-26

62. Maser RS, Monsen KJ, Nelms BE, Petrini JH (1997) hMre11 and hRad50 nuclear foci are induced during the normal cellular response to DNA double-strand breaks. Mol Cell Biol 17: 6087-96

63. Mizushima S, Nagata S (1990) pEF-BOS, a powerful mammalian expression vector. Nucleic Acids Res 18: 5322

64. Morgan WF, Day JP, Kaplan MI, McGhee EM, Limoli CL (1996) Genomic instability induced by ionizing radiation. Radiat Res 146: 247-58

65. Nowell PC (1976) The clonal evolution of tumor cell populations. Science 194: 23-8

66. O'Connell MJ, Walworth NC, Carr AM (2000) The G2-phase DNA-damage checkpoint. Trends Cell Biol 10: 296-303

67. Paciotti V, Lucchini G, Plevani P, Longhese MP (1998) Mec1p is essential for phosphorylation of the yeast DNA damage checkpoint protein Ddc1p, which physically interacts with Mec3p. Embo J 17: 4199-209

68. Pages V, Fuchs RP (2002) How DNA lesions are turned into mutations within cells? Oncogene 21: 8957-66

69. Parker AE, Van de Weyer I, Laus MC, Verhasselt P, Luyten WH (1998) Identification of a human homologue of the Schizosaccharomyces pombe rad17+ checkpoint gene. J Biol Chem 273: 18340-6

70. Paterson JW (1998) BRCA1: a review of structure and putative functions. Dis Markers 13: 261-74

71. Paulovich AG, Toczyski DP, Hartwell LH (1997) When checkpoints fail. Cell 88: 315-21

72. Peltomaki P (2001) DNA mismatch repair and cancer. Mutat Res 488: 77-85

73. Petrini JH, Bressan DA, Yao MS (1997) The RAD52 epistasis group in mammalian double strand break repair. Semin Immunol 9: 181-8

74. Powell SN, DeFrank JS, Connell P, Eogan M, Preffer F, Dombkowski D, Tang W, Friend S (1995) Differential sensitivity of p53(-) and p53(+) cells to caffeine-induced radiosensitization and override of G2 delay. Cancer Res 55: 1643-8

75. Prasher DC, Eckenrode VK, Ward WW, Prendergast FG, Cormier MJ (1992) Primary structure of the Aequorea victoria green-fluorescent protein. Gene 111: 229-33

76. Rauen M, Burtelow MA, Dufault VM, Karnitz LM (2000) The human checkpoint protein hRad17 interacts with the PCNA-like proteins hRad1, hHus1, and hRad9. J Biol Chem 275: 29767-71

77. Roos-Mattjus P, Hopkins KM, Oestreich AJ, Vroman BT, Johnson KL, Naylor S, Lieberman HB, Karnitz LM (2003) Phosphorylation of human Rad9 is required for genotoxin-activated checkpoint signaling. J Biol Chem 278: 24428-37

78. Rosen EM, Fan S, Rockwell S, Goldberg ID (1999) The molecular and cellular basis of radiosensitivity: implications for understanding how normal tissues and tumors respond to therapeutic radiation. Cancer Invest 17: 56-72

79. Rowley R, Subramani S, Young PG (1992) Checkpoint controls in Schizosaccharomyces pombe: rad1. Embo J 11: 1335-42

80. Russell KJ, Wiens LW, Demers GW, Galloway DA, Le T, Rice GC, Bianco JA, Singer JW, Groudine M (1996) Preferential radiosensitization of G1 checkpoint-deficient cells by methylxanthines. Int J Radiat Oncol Biol Phys 36: 1099-106

81. Sancar A (1994) Mechanisms of DNA excision repair. Science 266: 1954-6

82. Sanchez Y, Wong C, Thoma RS, Richman R, Wu Z, Piwnica-Worms H, Elledge SJ (1997) Conservation of the Chk1 checkpoint pathway in mammals: linkage of DNA damage to Cdk regulation through Cdc25. Science 277: 1497-501

83. Sasaki H, Chen LB, Auclair D, Moriyama S, Kaji M, Fukai I, Kiriyama M, Yamakawa Y, Fujii Y (2001) Overexpression of Hrad17 gene in non-small cell lung cancers correlated with lymph node metastasis. Lung Cancer 34: 47-52

84. Sausville EA, Arbuck SG, Messmann R, Headlee D, Bauer KS, Lush RM, Murgo A, Figg WD, Lahusen T, Jaken S, Jing X, Roberge M, Fuse E, Kuwabara T, Senderowicz AM (2001) Phase I trial of 72-hour continuous infusion UCN-01 in patients with refractory neoplasms. J Clin Oncol 19: 2319-33

85. Savitsky K, Sfez S, Tagle DA, Ziv Y, Sartiel A, Collins FS, Shiloh Y, Rotman G (1995) The complete sequence of the coding region of the ATM gene reveals similarity to cell cycle regulators in different species. Hum Mol Genet 4: 2025-32

86. Sherr CJ (1996) Cancer cell cycles. Science 274: 1672-7

87.   St Onge RP, Udell CM, Casselman R, Davey S (1999) The human G2 checkpoint control protein hRAD9 is a nuclear phosphoprotein that forms complexes with hRAD1 and hHUS1. Mol Biol Cell 10: 1985-95

88.   St Onge RP, Besley BD, Park M, Casselman R, Davey S (2001) DNA damage-dependent and -independent phosphorylation of the hRad9 checkpoint protein. J Biol Chem 276: 41898-905

89.   St Onge RP, Besley BD, Pelley JL, Davey S (2003) A role for the phosphorylation of hRad9 in checkpoint signaling. J Biol Chem 278: 26620-8

90.   Stillman B (1994) Smart machines at the DNA replication fork. Cell 78: 725-8

91.   Sun Z, Hsiao J, Fay DS, Stern DF (1998) Rad53 FHA domain associated with phosphorylated Rad9 in the DNA damage checkpoint. Science 281: 272-4

92.   Swift M, Reitnauer PJ, Morrell D, Chase CL (1987) Breast and other cancers in families with ataxia-telangiectasia. N Engl J Med 316: 1289-94

93.   Swift M (1994) Ionizing radiation, breast cancer, and ataxia-telangiectasia. J Natl Cancer Inst 86: 1571-2

94.   Swift M (1997) Ataxia telangiectasia and risk of breast cancer. Lancet 350: 740

95.   Tainsky MA, Bischoff FZ, Strong LC (1995) Genomic instability due to germline p53 mutations drives preneoplastic progression toward cancer in human cells. Cancer Metastasis Rev 14: 43-8

96.   Tauchi H, Matsuura S, Kobayashi J, Sakamoto S, Komatsu K (2002) Nijmegen breakage syndrome gene, NBS1, and molecular links to factors for genome stability. Oncogene 21: 8967-80

97.   Thelen MP, Onel K, Holloman WK (1994) The REC1 gene of Ustilago maydis involved in the cellular response to DNA damage encodes an exonuclease. J Biol Chem 269: 747-54

98.   Udell CM, Lee SK, Davey S (1998) HRAD1 and MRAD1 encode mammalian homologues of the fission yeast rad1(+) cell cycle checkpoint control gene. Nucleic Acids Res 26: 3971-6

99.   van der Burgt I, Chrzanowska KH, Smeets D, Weemaes C (1996) Nijmegen breakage syndrome. J Med Genet 33: 153-6

100.   Varon R, Vissinga C, Platzer M, Cerosaletti KM, Chrzanowska KH, Saar K, Beckmann G, Seemanova E, Cooper PR, Nowak NJ, Stumm M, Weemaes CM, Gatti RA, Wilson RK, Digweed M, Rosenthal A, Sperling K, Concannon P, Reis A (1998) Nibrin, a novel DNA double-strand break repair protein, is mutated in Nijmegen breakage syndrome. Cell 93: 467-76

101. Venclovas C, Thelen MP (2000) Structure-based predictions of Rad1, Rad9, Hus1 and Rad17 participation in sliding clamp and clamp-loading complexes. Nucleic Acids Res 28: 2481-93

102. Vialard JE, Gilbert CS, Green CM, Lowndes NF (1998) The budding yeast Rad9 checkpoint protein is subjected to Mec1/Tel1-dependent hyperphosphorylation and interacts with Rad53 after DNA damage. Embo J 17: 5679-88

103. Volkmer E, Karnitz LM (1999) Human homologs of Schizosaccharomyces pombe rad1, hus1, and rad9 form a DNA damage-responsive protein complex. J Biol Chem 274: 567-70

104. Waga S, Stillman B (1998) The DNA replication fork in eukaryotic cells. Annu Rev Biochem 67: 721-51

105. Wang Q, Fan S, Eastman A, Worland PJ, Sausville EA, O'Connor PM (1996) UCN-01: a potent abrogator of G2 checkpoint function in cancer cells with disrupted p53. J Natl Cancer Inst 88: 956-65

106. Weemaes CM, Hustinx TW, Scheres JM, van Munster PJ, Bakkeren JA, Taalman RD (1981) A new chromosomal instability disorder: the Nijmegen breakage syndrome. Acta Paediatr Scand 70: 557-64

107. Weinert T (1997) A DNA damage checkpoint meets the cell cycle engine. Science 277: 1450-1

108. Weinert T (1998) DNA damage and checkpoint pathways: molecular anatomy and interactions with repair. Cell 94: 555-8

109. Wood RD (1995) Proteins that participate in nucleotide excision repair of DNA in mammalian cells. Philos Trans R Soc Lond B Biol Sci 347: 69-74

110. Xu X, Weaver Z, Linke SP, Li C, Gotay J, Wang XW, Harris CC, Ried T, Deng CX (1999) Centrosome amplification and a defective G2-M cell cycle checkpoint induce genetic instability in BRCA1 exon 11 isoform-deficient cells. Mol Cell 3: 389-95

111. Yu Z, Chen J, Ford BN, Brackley ME, Glickman BW (1999) Human DNA repair systems: an overview. Environ Mol Mutagen 33: 3-20

112. Zakian VA (1995) ATM-related genes: what do they tell us about functions of the human gene? Cell 82: 685-7

113. Zou L, Elledge SJ (2001) Sensing and signaling DNA damage: roles of Rad17 and Rad9 complexes in the cellular response to DNA damage. Harvey Lect 97: 1-15

8 Abbreviations

α	Anti
APC	(familial) Adenomatous polyposis coli
APS	Ammonium polysulfide
AT	Ataxia telangiectasia
ATM	Ataxia telangiectasia mutated
ATR	Ataxia telangiectasia related
AU1	Australia antigen 1
BRCA1	Breast cancer 1
BSA	Bovine serum albumin
CaCl	Calcium chloride
CDK	Cyclin-dependent kinase
Chk1	Checkpoint kinase 1
CIP	Calf intestinal phosphatase
CsCl	Cesium chloride
DCC	Deleted in colon carcinoma
EDTA	Ethylenediaminetetraacetic acid
FCS	Fetal calf serum
FLAG	Flagellar antigen
G1	Gap 1 (in the cell cycle)
G1-S	Cell cycle boundary from G1 to S-phase
G2	Gap 2 (in the cell cycle)
G2-M	Cell cycle boundary from G2 to M-phase
GAA	Glacial acetic acid
GFP	Green fluorescent protein
GSH	Glutathione S-agarose
GST	Glutathione S-transferase
GTE	Glucose TRIS-EDTA
Gy	Gray
h	Human
HA	Hemagglutinin
HCl	Hydrochloric acid
HEPES	N-2-Hydroxyethylpiperazine-N'-2-ethanesulfonic acid
HRP	Horseradish peroxidase
Hus	Hydroxyurea-sensitive
Ig	Immuno-globulin
IR	Ionizing radiation
KAc	Potassium acetate
KCl	Potassium chloride
K_2HPO_4	Potassium phosphate
K-ras	Kirsten murine sarcoma virus oncogene causing rat's sarcoma
LB	Luria broth
LE Agarose	Low electroendosmosis agarose
LF	Li-Fraumeni
M	Mitosis
mAB	Monoclonal antibody
$MgCl_2$	Magnesium chloride

Microcystin-LR	Microcystin with leucin (L) and arginin (R) residues
NaAc	Sodium acetate
NaCl	Sodium chloride
NaF	Sodium fluoride
Na_2HPO_4	Sodium phosphate
NaN_3	Sodium azide
NaOH	Sodium hydroxide
Na_3VO_4	Sodium orthovanadate
NBS	Nijmegen breakage syndrome
OD	Optic density
p	Protein
$p53^-$	p53-deficiency
PAGE	Polyacrylamide gel electrophoresis
PCNA	Proliferating cell nuclear antigen
PCR	Polymerase chain reaction
PI-3	Phosphatidylinositol 3
PIK	Phosphatidylinositol 3-kinase
PIKK	Phosphatidylinositol 3-kinase-related kinase
PK	Protein kinase
PI	Propidium iodide
rad	Radiosensitive
RFC	Replication factor C
S	Synthesis
S.	Schizosaccharomyces
sc	Saccharomyces cerevisiae
sp	Schizosaccharomyces pombe
SDS	Sodium dodecyl sulfate
TAE	TRIS-acetate-EDTA
TB	Terrific broth
TBS	TRIS-buffered saline
TE	TRIS-EDTA
TEMED	Tetramethyl-1,2-diaminoethane
TP	Tumor protein
TRIS	Tris hydroxymethylaminoethane buffer
TWEEN 20	Polyoxyethylene sorbitan monolaureate
UCN-01	7-hydroxystaurosporine
um	Ustilago maydis
UV	Ultraviolet
XP	Xeroderma pigmentosum

9 Danksagung

10   Curriculum vitae

03.02.1974   Elias Volkmer, geboren in München

Schulische Ausbildung

1980 – 1984   Grundschule an der Nadistraße, München

1984 – 1993   Willi-Graf-Gymnasium, München

08.07.1993   Allgemeine Hochschulreife (Note 1,6)

Zivildienst

1993 – 1994   Integrationsförderung im Modellprojekt 27 e.V., München

Studium

1994 – 2001   Studium der Humanmedizin, Ludwig-Maximilians-Universität München

1995 – 1996   Universidad de Medicina, Alicante/Spanien, Erasmus-Stipendium

1996   Physikum (Note 2,3)

1997   1. Staatsexamen (Note 3,0)

1997 – 1998   Co-Assistent im Kursus der makroskopischen Anatomie

seit 1998   Doktorarbeit bei Prof. Dr. med. Dr. h. c. Gerd Plewig, Klinik und Poliklinik für Dermatologie und Allergologie der Ludwig-Maximilians-Universität München, und Dr. Larry Karnitz, Mayo Clinic, Rochester/Minnesota/USA

2000   2. Staatsexamen (Note 1,6)

2000 – 2001   Praktisches Jahr; Teilnahme am PJ-Austauschprogramm der *Harvard-Munich Alliance for Medical Education*

2001   3. Staatsexamen (Note 1,0; Gesamtnote 1,66)

Beruf

2001 – 2002   AiP in der Chirurgischen Klinik und Poliklinik, Klinikum Innenstadt, Ludwig-Maximilians-Universität München

seit 2003   Assistenzarzt der Chirurgischen Klinik und Poliklinik, Klinikum Innenstadt, Ludwig-Maximilians-Universität München

Publikationen

Volkmer E, Karnitz LM (1999) Human homologs of *Schizosaccharomyces pombe* rad1, hus1, and rad9 form a DNA damage-responsive protein complex. J Biol Chem 274: 567-570